Studies on Nucleic Acids – Structure and Dynamics

JOHAN ISAKSSON

Dissertation presented at Uppsala University to be publicly examined in Room C10:305 (floor 3), Biomedical Center (BMC), Uppsala, Friday, September 16, 2005 at 10:00 for the degree of Doctor of Philosophy. The examination will be conducted in English.

Abstract
Isaksson, J. 2005. Studies on Nucleic Acids – Structure and Dynamics. Acta Universitatis Upsaliensis. *Digital Comprehensive Summaries of Uppsala Dissertations from the Faculty of Science and Technology* 71. 75 pp. Uppsala. ISBN 91-554-6293-6.

This thesis is based on six papers, Papers I-VI, focusing on the interplay between the stabilizing elements of nucleic acids self-assembly; hydrogen bonding, stacking and solvent effects. In Paper I we investigate how the substitution of the O4' for CH_2 in the sugar moiety of adenosine (2'-deoxyaristeromycin) at the A^6 position of the Dickerson-Drew dodecamer makes the two modified bases exist in a dynamic equilibrium between Hoogsteen and Watson-Crick base pairing in the NMR time scale. Paper II is a structural study of the incorporation of 1-(1',3'-*O*-anhydro-*β*-D-psicofuranosyl)thymine in the T^7 position of the Dickerson-Drew dodecamer. NMR constrained molecular dynamics and hydration studies show the base-base distortions caused by the introduction of a North-type locked sugar in an otherwise B-type DNA•DNA duplex. Paper III shows that the stacking distortion caused by the 1-(1',3'-*O*-anhydro-*β*-D-psicofuranosyl)thymine building block perturbs the charge transfer similar to a DNA mismatch. Paper IV highlights how the sequence context affects the physico-chemical properties, monitored by the pK_a of guanine itself as well as how the charge perturbation is experienced by the neighboring bases, in ssDNA and ssRNA. Paper V focuses on the differences between the structural equilibria of single-stranded ssDNA and ssRNA. Directional differences in single-stranded stacking between ssDNA and ssRNA are identified and provide a basis to explain directional differences in pK_a modulation and dangling-end stabilization. In Paper VI the thermodynamic gains of dangling ends on DNA and RNA core duplexes are found to correlate with the X-ray geometries of dangling nucleobases relative to the hydrogen bonds of the closing base pairs.

Keywords: nucleic acids, modified nucleotides, NMR, structure, dangling-end, single-stranded, thermodynamics, hydration

Johan Isaksson, Department of Bioorganic Chemistry, Box 581, Uppsala University, SE-75123 Uppsala, Sweden

"In the year of 1492, the american indians discovered Columbus"
                                        -Martin Allwood

Till min Helen och mina Föräldrar

THE ORIGINAL PUBLICATIONS

This thesis is based on the following original publications, which are referred to by Roman numerals. Some related unpublished results are also included in the thesis.

I.   **Isaksson, J.**, Zamaratski, E., Maltseva, T. V., Agback, P., Kumar, A., and Chattopadhyaya, J. The First Example of a Hoogsteen Basepaired DNA Duplex in Dynamic Equilibrium with a Watson-Crick Basepaired Duplex –A Structural (NMR), Kinetic and Thermodynamic Study. *J. Biomol. Struct. Dyn.* **2001**, *18*, 783-806.

II.   **Isaksson, J.**, Plashkevych, O., Pradeepkumar, P. I., Pathmasiri, W., Petit, C., and Chattopadhyaya, J. Base-Base Distortions Introduced by Incorporating 3'-*endo*/4'-*exo* Locked-Sugar Containing Thymidine in a Self-complementary Dodecamer DNA - An NMR and MD Simulation Study. *submitted* **2005**.

III.   Boon, E. M., Barton, J. K., Pradeepkumar, P. I., **Isaksson, J.**, Petit, C., and Chattopadhyaya, J. An electrochemical probe of DNA stacking in an antisense oligonucleotide containing a C3'-*endo*-locked sugar. *Angew. Chem. Int. Ed.* **2002**, *41*, 3402-3405.

IV.   Acharya, S., Barman, J., Cheruku, P., Chatterjee, S., Acharya, P., **Isaksson, J.**, and Chattopadhyaya, J. Significant pK_a Perturbation of Nucleobases Is an Intrinsic Property of the Sequence Context in DNA and RNA. *J. Am. Chem. Soc.* **2004**, *126*, 8674-8681.

V.   **Isaksson, J.**, Acharya, S., Barman, J., Cheruku, P., and Chattopadhyaya, J. Single-Stranded Adenine-Rich DNA and RNA Retain Structural Characteristics of Their Respective Double-Stranded Conformations and Show Directional Differences in Stacking Pattern. *Biochemistry* **2004**, *43*, 15996-16010.

VI.   **Isaksson, J.**, and Chattopadhyaya, J. A Uniform Mechanism Correlating Dangling-end Stabilization and Stacking Geometry. *Biochemistry* **2005***, 44,* 5390-5401.

Contents

Abbreviations

A	Adenosine
C	Cytidine
DNA	Deoxyribonucleic acid
DSS	2,2-dimethyl-2-silapentane-5-sulfonate
G	Guanosine
H-bond	Hydrogen bond
HF	Hartree-Fock
LNA	Locked nucleic acid
N-type	North type
NMR	Nuclear Magnetic Resonance
MD	Molecular Dynamics
MM	Molecular Mechanics
MP	Møller Plasset basis set
mRNA	Messenger RNA
Np	Nucleoside, 3'-phosphate
pN	Nucleotide
PCR	Polymerase Chain Reaction
R	Pearson correlation coefficient
RNA	RiboNucleic Acid
RNAi	RNA interference
ROESY	Rotating frame nOe spectroscopy
rRNA	Ribosomal RNA
S-type	South type
siRNA	Short interfering RNA
ss	Single-stranded
T	Thymidine
tRNA	Transfer RNA
U	Uridine
UV	Ultra Violet
ΔG°	Gibbs free energy
ΔH°	Enthalpy
ΔS°	Entropy

1   Nucleic acids

Nucleic acids, DNA and RNA, are the fundamental carriers of information in the central processes in all living organisms. DNA is the long term storage medium of the genetic information, while RNA acts as the messenger (mRNA) between the genetic archive in the nucleus and the translation to proteins in the ribosome.

  In addition to the basic functionality as carriers of information, RNA can play many other important roles in the cell. The ribosomes are largely made up of RNA subunits (rRNA) and the delivery of the protein building blocks, the amino acids, to the ribosome is performed by transfer RNA (tRNA). RNA can actively take part in the processing of itself by a self-splicing mechanism, and specific sequences of both RNA and DNA can degrade other nucleic acid molecules in a multiple turnover process, acting as ribozymes and DNAzymes respectively.

  Further, nucleic acids are also the genetic transmitters in viruses. Viruses cannot only use DNA to store their genetic code - there are also RNA- and retroviruses that use RNA as the genetic carrier. The retrovirus family uses the Reverse Transcriptase (RT) that they carry in their genome to insert a DNA transcript (cDNA) of their RNA into the genome of the host upon a successful infection.

This thesis consists of studies on the structural- and dynamic properties of these complex multi-faceted molecules.

1.1   Configuration

Nucleic acids are polymers made up of nucleotide building blocks (*1-3*). The nucleotides in turn consist of three subcomponents: a nucleobase, a sugar moiety and a phosphate linker. The base is normally one of 9-adeninyl, 1-cytosinyl, 9-guaninyl or 1-thyminyl in DNA, while the 1-thyminyl is replaced by 1-uracilyl in RNA (Figure 1). A single group, the 2' hydroxyl, in the sugar moiety distinguishes RNA (2'-β-D-ribofuranosyl) from DNA (2'-β-D-deoxyribofuranosyl). This seemingly subtle difference between DNA and RNA gives rise to the very different functions of these two groups of molecules, which will be further discussed below. The nucleoside building blocks are covalently linked by a 3', 5'-phosphodiester group, completing the assembly of the single-stranded oligonucleotide (Figure 1).
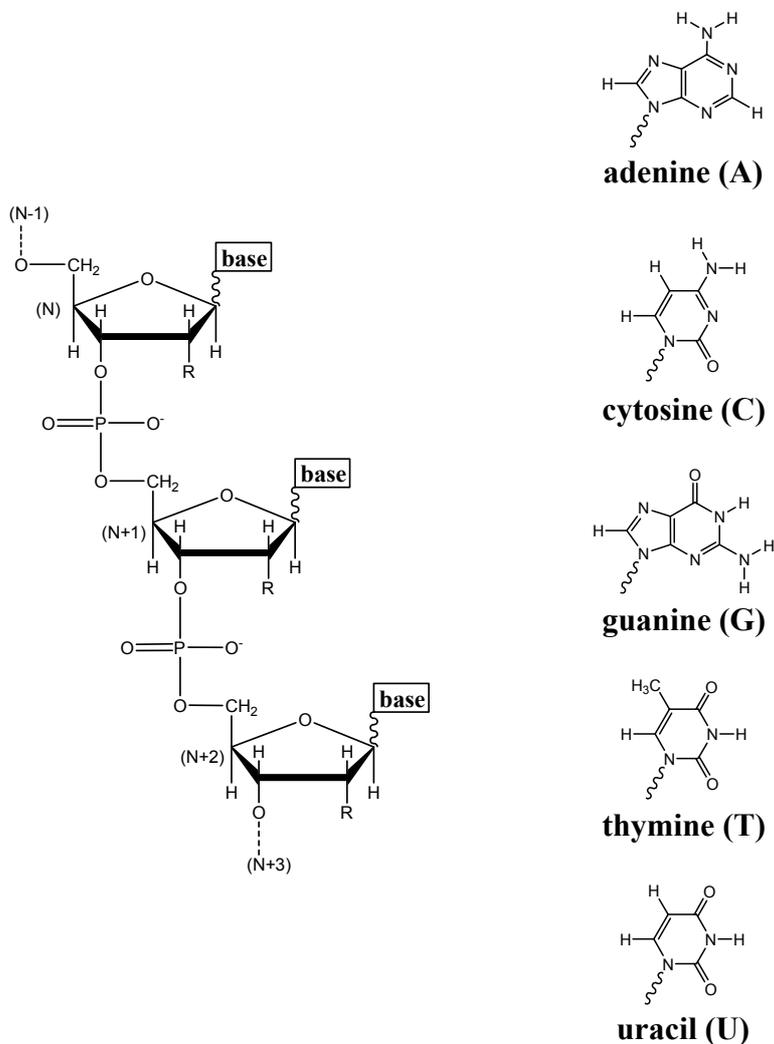
Figure 1. Schematic representation of the configurations of DNA and RNA. DNA: R = H, β-D-2'-deoxyribofuranosyl, base = A, C, G or T and RNA: R = OH, β-D-2'-ribofuranosyl, base = A, C, G or U.

1.2 Self-assembly

The ground breaking double helical model of DNA structure was first proposed by Watson and Crick in 1953 (*4*), based on the earlier observations that the A:T and G:C ratios always are unity (*5*) and the solved crystal structure of 5'-deoxycytidine (*6*), that revealed the fundamental

10

conformation of the nucleoside: the planarity of the nucleobase and the puckered conformation of the sugar moiety. It was correctly deduced that G forms base pairs exclusively with C and that A forms base pairs exclusively with T (or U in RNA), and that the two strands wind around each other in opposite directions like a spiral staircase forming a anti-parallel double helix structure (Figure 7). The stabilization of the nucleic acid duplex structure has classically been described (3) as the sum of the stacking interactions between the parallel nucleobases, the cross-strand base pairing interactions between the nucleobases and the electrostatic repulsion of the phosphate groups. Other factors that affect the formation of the duplex structure are the degree of pre-organization of the single strands (7), condensation of counter-ions around the backbone (8, 9) and solvent effects (hydration and hydrophobic effects).

1.2.1   Hydrogen bonding

Hydrogen bonding is the major (possibly the only) attractive force that acts *across* the two strands in nucleic acids to *directly* stabilize the double-stranded complex. With the possible exception of some degree of inter-strand stacking, the other contributors to duplex stability that are traditionally acknowledged (1-3) are either of entropic nature (freezing internal motions, complex formation and solvent entropy) or factors modulating the strengths of the hydrogen bonds (stacking dehydration and charge dispersion) or the phosphate-phosphate repulsions (counter-ion condensation, hydration).

  IR and NMR studies of monomer nucleobase derivatives in organic solvents have shown that even in the absence of the sugar-phosphate backbone they form hydrogen bonds with a high specificity of correct base pairs (G·C and A·T/U) relative to self-association and mismatched base pairs (10-12). These results have some significance also in aqueous solution since the interior of the double-stranded nucleic acids are relatively devoid of water. Hydration studies from our laboratory (13) and others (14-19) have displayed that the exchange rate is reduced in the core of the duplex compared to the ends, and that the introduction of a mismatch hydrates the structure (13, 16). It has further been shown that the attachment of a 5'-phenazinium tether to both matched and mismatched duplexes reduce their respective internal hydration (20). Becker *et al* (21) has also elegantly demonstrated that acridinium ester has a significantly lower hydrolysis rate inside a

complementary double helix compared to the inside of a mismatched duplex.

The unique base pairing ability of the four native nucleobases comes from their electrostatic complementarity. The charge densities and dipole moments of the nucleobases determined by X-ray diffraction (*22*) as well as theoretic calculations (*23-26*) show that the nucleobases have highly characteristic potential energy surfaces in the plane of the base, in such a way that the complementary bases can interact like an electrostatic jigsaw puzzle (Figure 2). It should however be noted that the stability of a base pair is not perfectly proportional to the number of hydrogen bonds at monomer level (*11, 12, 27, 28*). It has been argued for (*26, 29*) and against (*30, 31*) the importance of non-linear secondary hydrogen bond interactions between atoms on the faces of the nucleobases. The exact nature that determines the stability of a base pair is still unclear, but it appears that the cumulative electrostatics of the entire base is important.

| 9-adeninyl | R = H (1-uracilyl), CH$_3$ (1-thyminyl) | 9-guaninyl | 1-cytosinyl |
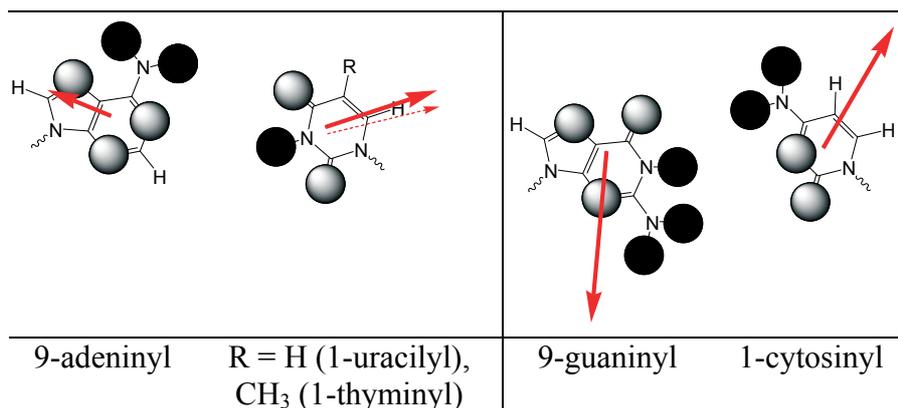
Figure 2. Schematic representations of the atoms' ability do act as donors (black) and acceptors (white) at hydrogen bond formation. The arrows represents the dipole moments (at the MP2/aug-cc-pVDZ level) (*23*) of the isolated bases (solid arrow: thymine, broken arrow: uracil).

In addition to the native Watson-Crick base pairs (*4*), G·C and A·T/U (referred to as canonical base pairs), several unusual base pairing modes involving different donor/acceptor atom combinations are possible (*1, 2, 32*) (non-canonical base pairs). For example, structural studies have discovered naturally occuring A·T Hoogsteen-, G·C reverse Watson-Crick-, G·U and G·T wobble- and A·G base pairs in yeast tRNA[Phe] (*1, 33, 34*), and A·U Hoogsteen- and A·G base pairs have been found in ribosomal RNA (*35, 36*). It is also known that Hoogsteen base pairing is crucial in triplex (*37-42*) and tetraplex (*43-*

49) formation, and that ionized bases can engage in unusual base pairs (*50-56*).

   It has been established that the strength of a hydrogen bond is proportional to the dielectric constant of the solvent (*57, 58*). A common mechanism of enzymatic catalysis is proposed to be that the microenvironment in the interior of the enzyme has a much lower dielectric constant than the surrounding solvent, making the hydrogen bond mediated stabilization of the transition state much stronger inside the active site than free in solution, thereby catalyzing the reaction upon substrate binding. The hydrogen bonds in double-stranded complementary duplexes function in a very similar way. An optimally stacked oligonucleotide effectively dehydrates (*21*) the microenvironment of the hydrogen bonds, enabling the formation for strong hydrogen bonds. The incorporation of a mismatch, or any other distortion, into a duplex structure however disturbs the stacking pattern so that the hydrogen bonds of the base pairs at the site of distortion become more exposed to the bulk water, weakening the strength of the double-strand complex.

1.2.2   Stacking

Stacking interactions in general (*59*) (aromatic-aromatic interactions) are of fundamental interest in molecular recognition and the folding of virtually all biological systems.
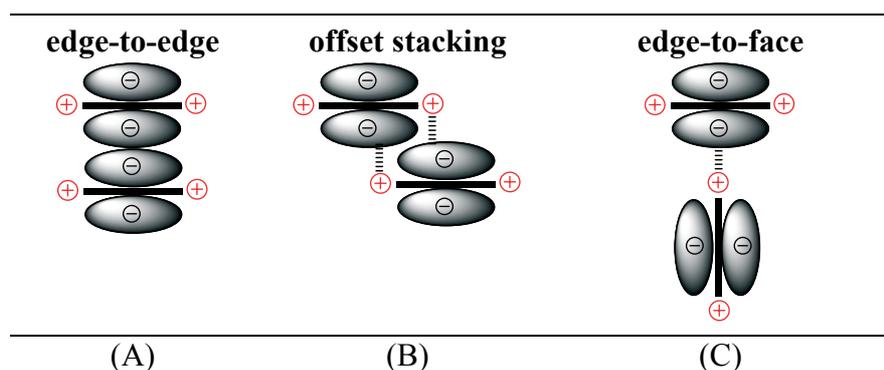

| (A) | (B) | (C) |

Figure 3.   Schematic cross-section of two aromatic rings in (A) edge-to-edge stacking, (B) offset stacking and (C) edge-to-face stacking (T-shaped). The π-electron ring is represented by a negative sphere and the electron-deficient σ-frame is represented by a positive point charge.

One of the most obvious roles is the stacking interactions between the nucleobases in nucleic acids duplex structures that complement the base pairs in giving nucleic acids their unique specificity and stability.

Stabilizing π-π (*60, 61*), CH-π (*62-66*), ion-π (*67-71*) interactions have been identified and estimated in aromatic model systems and are all potentially important in nucleic acid duplex stabilization. However, studies on substituted 1,8-diarylnaphthalenes suggest that the $\pi-\pi$ interaction is mainly repulsive in nature and that the interaction between the rings is favored by lower electron density (*72, 73*). This strongly implies that the electron distributions of the nucleobases directly steer the preferred stacking geometries in a sequence specific manner, not only by *attractive* electrostatic- and dispersion interactions, but also by the minimization of the *repulsions* between the bases.

X-ray crystallographic charge densities have been used to construct energy maps based on van der Waals and electrostatic interactions for stacked DNA nucleobases (*74*). The importance of offset stacking (Figure 3) in DNA, in which the partial atomic charges of one base pair interacts with the π-electron density of a neighboring base, is identified. This study further suggests that the strong dipole moments of the G and C nucleobases (Figure 2) are responsible for the preference of the strongly slided conformations associated with A-DNA and the left-handed Z-DNA (Figure 7) by G-C rich sequences.

1.3 Conformations

1.3.1 Pseudorotation

Fully planar conformations of five-membered rings are energetically very unfavorable (*75*) and are normally not populated. The intramolecular strain of the planar conformation is therefore spontaneously released by dislocating one of the ring atoms out of the plane, forming a relaxed puckered ring structure. The pseudorotation concept (*76*) (Figure 4) can be used to describe the conformation of the ribose and deoxyribose rings in nucleosides and nucleotides with two variables, the pseudorotation phase angle (P) and the puckering amplitude (Φ_m) (*77-79*). The phase angle describes which part of the ring that is mostly displaced from the plane made up by the other four ring atoms,

while the puckering amplitude describes the maximum angle between the puckering atom and the plane.

For nucleic acids, the twist form 3'-*endo*, 2'-*exo* is chosen as standard conformation ($P = 0°$), and hence the mirror conformation, 2'-*endo*, 3'-*exo* is found opposite in the pseudorotation wheel ($P = 180°$). The shaded area in Figure 4 shows the commonly populated (based on 60 solved X-ray structures of β-nucleoside derivatives) sugar conformations in native DNA and RNA (*77-79*), the 2'-*endo* and the 3'-*endo* conformations respectively. Conformations that lie within the top hemisphere of the psudorotation wheel are often referred to as North conformations while conformations that lie within the lower hemisphere are referred to as South conformations.
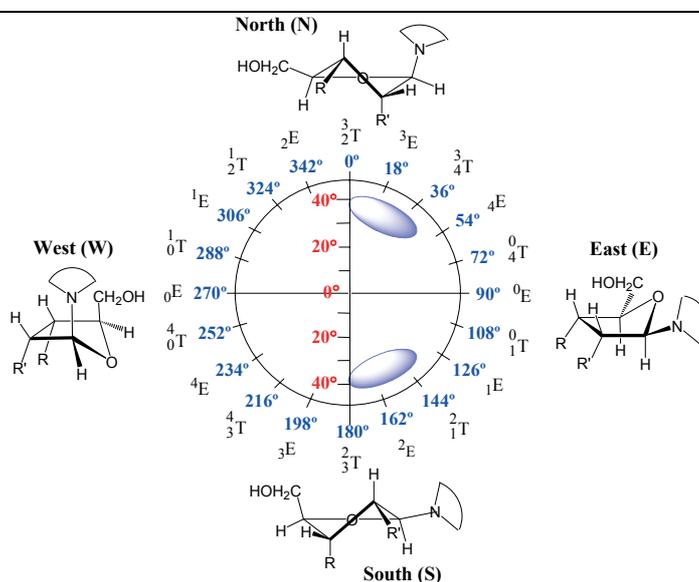
Figure 4. The pseudorotation wheel for the ribose and deoxyribose rings in nucleic acids. The phase angle, P, is represented around the circle and the puckering amplitude, Φ_m, is represented on the axis. The North-type and South-type pseudorotamers commonly populated in β-D-oligonucleotides are shaded (*77-79*).

1.3.2   Backbone torsions

The sugar-phosphate backbone conformation can be described by a series of torsion angles that are defined according to the IUPAC recommendations (*80*), illustrated in Figure 5. These torsion angles are often roughly described as being in a conformational region, rather

than being exactly defined. The Klyne-Prelog nomenclature is recommended (*81*) for this purpose, *i.e. syn* = 0 ± 90º, *anti* = 180 ± 90º with the subregions ± synperiplanar (± *sp*, 330-30º), ± synclinal (± *sc*, 30-90º and 270-330º), ± anticlinal (± *ac*, 90-150º and 210-270º) and ± antiperiplanar (± *ap*, 150-210º). Other descriptions that are commonly used to describe certain values of torsion angles are *cis* (0º), *trans* (180º), + *gauche* (60º) and – *gauche* (300º).
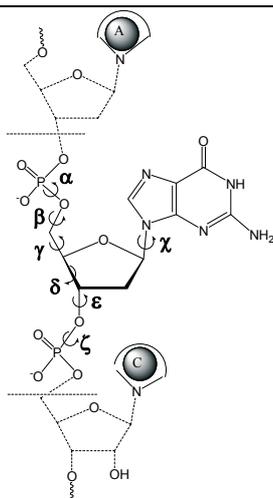
Figure 5. The definition of the torsion angles describing the sugar-phosphate backbone conformation of oligonucleotides.

Statistical surveys of solved X-ray structures of both nucleotides (*82*) and oligomer duplex structures (*83*) have shown that all torsion angles, except the γ torsion in monomers, are correlated (R = 0.65-0.89) (*1*) with each other to some extent. Thus, all conformational transitions in helical structures must be considered to be simultaneous concerted motions of all torsion angles.

1.3.3 Helical parameters

The three-dimensional arrangements of the bases and base pairs in oligonucleotide duplexes are described by a set of parameters that relate each residue to a local helical axis. A standard reference frame for these parameters has been developed by Olson et al. (*84*) in order to synchronize the use of different structure analysis software, for example CompDNA (*85, 86*), Curves (*87*), RNA (*88*) and 3DNA (*89*).

16

The relative positions and orientations of two complementary bases in a base pair are defined by the six complementary base pair parameters - the translational base pair parameters (Figure 6A): shear, stretch and stagger, and the rotational base pair parameters: opening, buckle and propeller. The stacking geometry of a base pair step is described by six parameters (Figure 6B): shift, slide, rise, tilt, roll and twist. The additional six local helical parameters (Figure 6C): x-displacement, y-displacement, helical rise, inclination, tip and helical twist, describe the regularity of the helix.
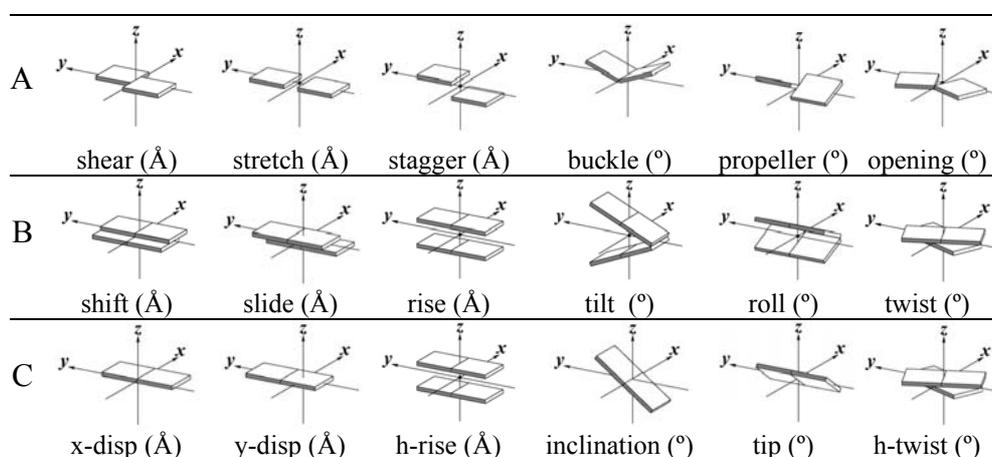
Figure 6. Definitions of the (A) complementary base pair parameters, the (B) base pair step parameters and the (C) local helical parameters.

Another important helical feature that describes the duplex form is the minor- and major groove widths and depths. The groove widths are defined as the shortest distance between the backbones of the two strands. The shortest distance from each phosphate group to any phosphate on the opposite strand, minus 5.8 Å corresponding to the van der Waals radii of the phosphate groups, is used for reference. The minor groove is defined as the side of the base pairs facing the sugar phosphate backbone and the major groove is facing the opposite direction. The depth of the minor groove is defined as the distance from the phosphate to the N2 of G, the N3 of A or the O2 of C and T, minus the sum of the van der Waals radii (1.4 for oxygen, 1.5 for nitrogen) while the depth of the major groove is defined as the reduced distance between the phosphate and the O6 of G, N6 of A, O4 of T or N4 of C (*90*).

1.3.4 Canonical conformations

It was early discovered that the fiber diffraction patterns of nucleic acids in addition to the sequence context also vary depending on environmental factors like salt concentration, crystal humidity, choice of counter-ions and solvent (*91-93*). The polymorphism of nucleic acids due to external factors reflects its responsiveness to interactions with cellular enzymes, regulatory factors or packing proteins.

A-DNA	B-DNA	Z-DNA
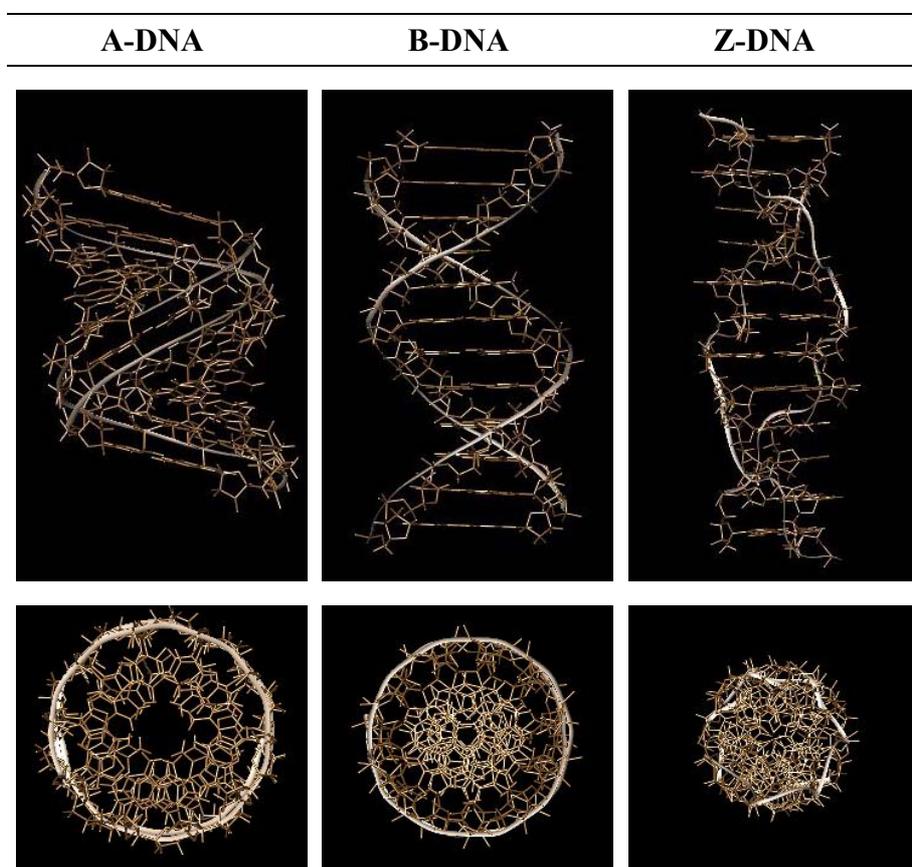
Figure 7. Side- and top projections of the canonical A-, B- and Z-forms of DNA. Ribbons are added to the backbones, highlighting the differences minor- and major groove widths of the different canonical forms.

Following the first solved nucleic acid single crystal structure (*94*), structures with different diffraction patterns have been solved (*95*), revealing the structural characteristics of the most common conformations, the A-, B- and Z forms of DNA (Figure 7).

DNA oligomer structures are categorized into different families depending on their helical characteristics, where the most distinguished are the A- B- and Z- forms, while RNA mainly exists in the A-form. The A- and B- forms can consist of any sequence but is sensitive to the degree of hydration and the nature of counterions, while the conformationally distinguished left-handed Z-form is always made up by (pyrimidine-purine)$_n$ tandem repeats of alternating conformation. The major distinguishing features in the A-, B- and Z-forms are summarized in Table 1.

Table 1. Some average helical parameters that are distinguishing the A-, B- and Z-forms of DNA (*2*).

	A-form	*B-form*	*Z-form*
Helicity	*right*	*right*	*Left*
Base pairs per repeat	1	1	2 (*pyr;pur*)
Base pairs per turn	11	10	12
Sugar conformation	3'-*endo*	2'-*endo*	2'-endo;3'-*endo*
Glycosidic bond (χ)	*anti*	*anti*	*anti;syn*
Minor groove Width (Å)	11.0	5.7	4
Depth (Å)	2.8	7.5	9
Major groove Width (Å)	2.7	11.7	*convex*
Depth (Å)	13.5	8.5	*convex*
Helix rise (Å)	2.9	3.4	-3.9;-3.5
X-displacement (Å)	-4.1	0.8	3.0
Helix twist (°)	32.7	36.0	-10;-50
Inclination (°)	12	2.4	-6.2

The common feature of all solved nucleic acid structures is the constant high degree of stacking between neighboring bases. Thus, it is safe to assume that efficient base-base overlap is a pre-requisite for stable duplex formation.

Either of the two major right-handed structural families, the A- and B-forms, is generally adopted by a random sequence DNA. The fundamental difference between the A- and B-forms is the position of the base pairs relative to the helix axis, as reflected by their respective X-displacements in Table 1, as well as the average phase angles of the sugars, resulting in very different groove widths. The A-form is gen-

erally favored by high G-C content, lower relative humidity and high concentrations of salt (*96, 97*). The barrier between the A- and the B-form is however relatively low as there are even reports of a sequence, d(GG^{Br}UA^{Br}UAAC), that co-exist in A- and B-forms within a single crystal lattice (*98*).

Z-DNA is favored by high salt concentrations (*99-101*) and is only formed under very specific sequence conditions of certain alternating pyrimidine-purine tandem repeats. For example, (dC-dG)$_n$ and (dA-dC)$_n$ repeats are known to be able to adopt Z-form while others such as (dA-dT)n and (dC-dG)$_2$-(dT-dA)-(dC-dG)$_2$ can not (*102*).

1.4 Hydration

One can not consider nucleic acids structure and function without taking the surrounding water into account as it is present in very high concentrations (~55 *M* in the cell) in all biologically important interactions involving nucleic acids. Water has some unique features as a solvent originating from the large difference in electronegativity between the oxygen and hydrogen atoms, together with the asymmetric angle between the hydrogen atoms (~105°) (*103*). The oxygen has a partial negative charge ($q_O \sim$ -1.8 eu) and the hydrogens have a partial positive charge ($q_H \sim$ +0.5 eu), giving the molecule a large electric dipole moment (μ = 1.85 D). Thus, water efficiently forms hydrogen bonds with it self and with hydrogen bond donors (H) and acceptors (mainly N and O) on nucleic acids and other biological molecules. The enthalpy gain in stabilization is balanced by an unfavorable decrease in entropy as the motional freedom of the water molecules becomes restricted upon hydrogen bond formation. The high dipole moment of water results in a high dielectric constant (ε = 78), which in turn makes Coulombic interactions weaker in water ($E = q_1 \, q_2 / 4\pi \varepsilon r$) than in organic solvents (compare DMSO, ε = 48). Thus, ions, as well as the highly charged nucleic acids, are effectively solvated in water.

Many studies have been performed on DNA in order to determine the extent of specifically bound water. Between 7 and 12 water molecules per residue are reported as *tightly* associated in the first shell of hydration of the nucleic acid by IR spectroscopy (*104, 105*), gravimetry (*106*), hydrodynamic- (*107, 108*) and unfrozen water (*105, 109, 110*) methods. The IR studies have also resulted in a ranking of which of the possible sites that are preferably hydrated as the relative humid-

ity in the sample is gradually increased. The order in which different energy transition bands are affected by the water content leads to the conclusion that the ionic phosphates are most strongly hydrated at very low levels of relative humidity, followed by the phosphodiesters and furanose oxygens (*104*). The bases are least hydrated – the bands of the carbonyls and heterocyclic nitrogens only start to shift at a relative humidity above 65%.

  The trapped water molecules in X-ray structures have also been used to draw conclusions about the hydration of nucleic acids. A spine of hydration running in the minor groove in the AT-rich core was first identified in the Dickerson-Drew dodecamer sequence, d(CGCGAATTCGCG)$_2$ by X-ray crystallography (*111, 112*) and later confirmed by NMR (*113, 114*) to have a residence time in the nanosecond regime. More recent high resolution structures (*115-120*) have evolved this picture further. Comparison of the hydration patterns of sequences with different minor groove widths reveal that the spine is characteristic of narrow groove widths (~4 Å) while a dual ribbon pattern is found in sequences with wider minor groove widths (~7 Å). Intermediate minor groove widths have no ordered hydration pattern and only sparse clusters of ordered water reside in the major groove and around the phosphate groups. The fact that all exposed hydration sites exhibit more disorder (*111, 112*) (and thus are harder to detect) than narrow pockets may indicate that a steric fit is necessary to restrict the entropy of the resulting hydration pattern in addition to the aligning electrostatics in order to detect them in crystallography.

1.5 Dynamics

The mobility of nucleic acids can be divided into two categories, the local motions and the large-scale motions. The local motions consist of flexible atoms or moieties of the nucleic acids. The sugar moieties, especially in DNA where the stabilizing 2'-OH effects are absent, exist in an fast equilibrium between North and South conformations (section 1.5.1) and the entire sugar-phosphate backbone is flexible, making it possible for bases to destack and stack, breaking and reforming the base pair (section 1.5.2). The large-scale motions are the macroscopic sums of the local structural flexibility and consist of helix bending, supercoiling and unwinding.

1.5.1 North-South equilibrium

Computational simulations (*121-130*) at different theory levels as well as experimental studies (*131, 132*) of nucleosides/nucleoside mimics reveal that the potential energies of the 3'-*endo* and 2'-*endo* sugar conformations are nearly equivalent ($\Delta G < 0.4$ kcal/mol), separated by an energy barrier of 1.2 to 5.0 kcal/mol traced through the *East*-type O4'-*endo* conformation (Figure 8). However, most of the older studies use constant puckering amplitude based on crystal structures in their calculations, thereby increasing the resulting energy barrier. Recent theoretical calculations (*126, 130*) of 2'-deoxynucleosides based on the stochastic difference equation algorithm (*133*) as well as the MP2/6-31G* theory level are more in agreement, reporting energy barriers for furanose interconversion of ~2 kcal/mol. In other recent work, simulations of solid state deuterium NMR line shapes (*131*) of [2"-^{2}H]-2'-deoxycytidine at the C^3 position in the Dickerson-Drew dodecamer, d(CGCGAATTCGCG)$_2$ suggest an energy barrier of 3.3 kcal/mol. The reduced conformational freedom of the nucleobase in this work (where the nucleoside is incorporated inside a fully complementary duplex structure), compared to the simulations of the free nucleosides, most likely accounts for the 1 kcal/mol higher effective energy barrier.

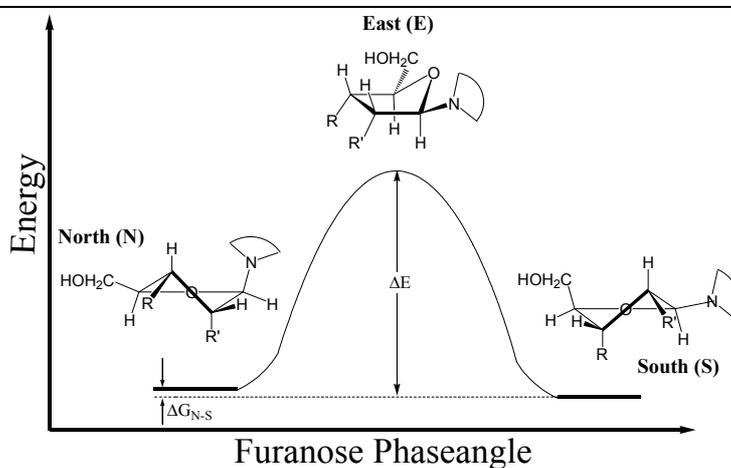*Figure 8.* Schematic representation of the two-state North ⇄ South model. The potential energy difference between the North and South minima (ΔG_{N-S}) is very small and the two energy wells are separated by an energy barrier (ΔE) of ~2 kcal/mol.

The relatively low energy barrier leads to rapid transitions between the two low energy conformations at room temperature (*134, 135*). Hence, the sugar conformation is often treated as a two-state equilibrium of the North⇄South conformations. The average sugar conformation is determined by a delicate balance between steric-, anomeric- (*136-142*) and *gauche (128, 137, 138, 140, 142-146)* effects. The nucleobase promoted anomeric effect drives the sugar towards the North-type conformations, where the stabilizing $n_{O4'} \rightarrow \sigma^*_{C1'-N1/9}$ orbital mixing is feasible (*140*). The anomeric effect is balanced by the steric- and *gauche* effects, which drive the sugar towards South-type conformations in DNA. There is less steric competition between the nucleobase and the sugar when the nucleobase takes up a pseudo-equatorial orientation, which is the case when the sugar is in South conformation. The *gauche* effect in DNA further stabilizes the South over the North conformation through the $\sigma_{C3'H3'} \rightarrow \sigma^*_{C4'O4'}$ orbital overlap. In RNA, the addition of the 2'-OH creates possibilities for two new *gauche* interactions, the O2'→O4' and O2'→N9/N1 overlaps (*139*). The sum of these two possible interactions together with the steric effects of the 2'-OH gives a net shift in stabilization towards North type conformations in RNA compared to DNA.

The North⇄South equilibrium can be tuned towards either conformation by several methods. The nature of the nucleobase (*i.e.* the electron density at the N1/N9) will affect the strength of the anomeric effect in the following order: C > U/T > A > G (*140*). Protonation/deprotonation (*139*) as well as any substituents (*147, 148*) that affect the charge distribution of the base (*139-141*) will steer the sugar conformation accordingly. Similarly, electronegative substitutions on the furanose can reinforce existing *gauche* effects (*146, 149, 150*) or create new ones (*149-151*). Further, environmental factors like salt condensation, relative humidity and solvent, as well as the nucleobase sequence, can affect the preferred sugar conformation. This is achieved either through charge neutralization affecting the charge distribution through specific hydration of the phosphates, stabilizing either the A- or B-form via inter-phosphate distances, or through preferential stacking due to the sequence steering the sugar conformation via the χ torsion.

The delicate balance between all these factors gives nucleic acids their biologically essential structural polymorphism and responsiveness to the surrounding medium, other macromolecules or nucleic acid binding molecules.

1.5.2   Nucleobase dynamics

The lifetimes of imino protons in water have been used to probe the large amplitude motions: opening and closing of individual base pairs in double-stranded DNA (*13, 17, 18, 152-157*) and RNA (*18, 158-162*) by ^{1}H NMR. Using base catalysis to ensure that the opening rate is the rate limiting step for the imino proton exchange, the opening rate of base pairs in nucleic acids in solution is determined to reside in the millisecond to microsecond regime below room temperature (*13, 18, 155, 157*).

It has also been found that the nucleobases in DNA and RNA exhibit dynamics with a correlation time in the low nanosecond scale by electron spin resonance (ESR) spectroscopy (*163-165*) and ^{1}H NMR relaxation (*166*). The RNA r(CGCGAAUUCGCG)$_2$ (*167, 168*) duplex and the corresponding DNA (*169*) duplex have also been studied by solid-state ^{2}H NMR. The motions of the purines in both duplexes are best simulated by a *restricted motion on a cone* model with small amplitudes (< 10°) and rates in the nanosecond scale at low levels of hydration to the microsecond scale at high levels of hydration.

Further, the internal dynamics of tRNA has been studied by depolarized dynamic light scattering (DDLS) (*170*), where the authors conclude that the fast internal base motions take place in clusters of approximately five residues.

2   Modified nucleotides in DNA

Using oligonucleotides as therapeutic molecules is a very appealing thought. Firstly, the highly sequence specific interactions between complementary strands would make it possible to direct an oligonucleotide against any known pathogenic gene, thus talking directly to the cell using its own language. Secondly, oligonucleotides are built up by monomer building blocks, making it possible to target a billion different sequences using only a 15mer consisting of four building blocks in different combinations. If this targeting potential can be effectively combined with a therapeutic response, efficient delivery and increased stability *in vivo*, without introducing toxic side effects, this approach have the potential to be usable as a multi-purpose gene knock-out therapy.

2.1   Gene silencing

Antisense is a broad term that is used to describe interference of RNA during its processing from mRNA to protein or its other active functions, like splicing, translational arrest and degradation of mRNA (*171-173*). Gene silencing by the antisense approach can go through one of several mechanisms. (1) By binding strongly to the target mRNA, the antisense oligonucleotide can block the translation of the mRNA. (2) Through the formation of an antisense DNA·mRNA hybrid that recruits RNase H (*174-176*), an enzyme that specifically degrade the RNA strand of DNA·RNA hybrid duplexes. (3) The antisense oligonucleotide itself can have enzymatic activity in the form of a DNAzyme (*177-180*) or ribozyme (*181-183*).

  Although the antisense strategy is very elegant in its approach, the method has several drawbacks. The main obstacle is that single-stranded nucleic acids are quickly digested in the cell, mainly by $3' \rightarrow 5'$ exonucleases (*184*), not only reducing the potency of the antisense treatment, but also producing potentially toxic levels of nucleoside monophosphate digestion products (*185*). The other problem is to efficiently deliver the antisense strand into a variety of cell types, as nucleic acids are both too large and too polar (even in the absence of its negatively charged phosphate backbone) to pass the cell membrane by passive diffusion (*186*).

  In order to overcome these problems, various chemical modifications to the sugar-phosphate backbone have been evaluated for their potency as antisense agents. Apolar modifications were first studied.

Methyl substitution of one of the non-binding oxygens of the phosphodiester link resulted in the methylphosphonate oligodeoxynucleotides who, are almost invulnerable to nuclease digestion but with reduced antisense activity and cellular uptake (*187*). Other uncharged species like peptide nucleic acids (PNA) (*188-190*) and morpholino-oligomers (*191-193*) displayed the same inability to adhere to the cell surface for active transport into the cell by endocytosis. These and many other backbone modifications have been comprehensively reviewed by Micklefield (*173*). The next development was the polar phosphorothioate oligodeoxynucleotides (*194, 195*), arabinonucleic acids with- and without 2'-fluoro substitution (ANA and 2'F-ANA) (*196*) and locked nucleic acids (LNA) (*197-201*), as well as the oxetane locked nucleic acids (*202-208*) studied in this laboratory. These compounds display increased resistance against nucleases compared to native oligonucleotides, and maintain sufficient solubility in aqueous media and efficiency of cellular uptake (*209*). There are several formulations in clinical trials and one of them, Vitravene® (Fomivirsen), has as the first oligonucleotide drug been approved by the FDA, Rockville, MD (*210*) for treatment of CMV retinitis. The most promising candidate for further approval is Genasense®, which is in phase 3 clinical trials for several cancer treatments. The phosphorothioates are however highly biologically active molecules and pronounced toxic side-effects have been reported (*211-214*), mainly associated with non-specific binding to cellular proteins, like growth factors or their receptors (*212, 213, 215*), laminin (*216*), Mac-1 (*217*), CD4 (*218*), reverse transcriptases (*219*) and DNA polymerase/RNase H (*220*).

Another problem with antisense is the "irrelevant cleavage" by RNase H (*221, 222*). It has been shown that only 4-8 complementary base pairs between DNA and RNA are required to induce RNase H cleavage, and that cleavage can occur in partly base paired sequences. This has the side effect that the longer a sequence is, the more possibilities there are for partial complementarity to sequences not originally targeted by the oligo in its full length promoting unspecific cleavage. Therefore, modified nucleic acid analogues that bind more strongly to the target make it possible to use shorter sequences, and more importantly, analogues that cannot recruit RNase H when used in a homogenously modified oligomer can be used in mixed oligonucleotides (*223*) (sometimes referred to as second generation antisense), or gapmers, leaving 6-8 native nucleotides as an active RNase H window and modified strongly binding recognition arms to increase binding affinity without opening up for unspecific RNase H cleavage.

26

The LNA approach has recently presented promising results where LNA bind potently in biological media (*224*) and outperform the corresponding native forms of both DNAzyme (*225*) and triplex forming oligodeoxynucleotides (*226, 227*). The *c-myb* gene expression has successfully been reduced deploying an oxetane locked nucleic acid analogue from our laboratory (*206*) in a molar potency that exceeds the corresponding phosphorothioate (*203*).

Even though very promising *in vitro* results have been presented, the success rate *in vivo*, particularly in higher mammals, have left much to wish for. The combination of different nucleoside analogues into designed "mixmers" breaths some optimism on the construction of potent specific antisense compounds without toxic side effects. Hence, research on novel building blocks that can complement the existing arsenal is important in order to advance the field further.

A more recent strategy of gene silencing is achieved through RNA interference (RNAi) (*228-231*) by small RNAs, including microRNAs (miRNA) and short interfering RNAs (siRNA). The siRNAs have a double-stranded form and act as a template for specific degradation of complementary free mRNA in a RNA-induced silencing complex (RISC) composed of several cellular proteins in eukaryotes, as a natural defense against viral RNA.

Another related mechanism is the antigene effect, in which the antigene oligonucleotide binds directly to the gene in the dsDNA, either by out-competing the native complementary strand and sterically blocking transcription (gene invasion), or by triplex or quadruplex formation at a regulatory position of the target gene (*232*). Locked nucleic acids have successfully been deployed to control the folding of a quadruplexes (*233*), which may be exploitable in this approach.

2.2 Diagnostic applications

The application of chemically modified nucleic acids in diagnostics and biotechnology is much more straightforward, as toxicity and delivery are no issues. Conformationally restrained nucleotides have been successfully used in several fields. LNAs have been used to increase the discrimination of single-nucleotide mismatch detection (single-nucleotide polymorphism, SNP) in PCR/fluorescence assays (*234*) and they have outperformed routinely used minor groove binder probes (*235*) and native DNA probes (*236*) in 5'-nuclease PCR assays.

The strong affinity of LNA for hybridizing to RNA has also been exploited in mRNA capture probes for poly-A sequences (*237*). The same principle can be used to design highly efficient micro arrays (*238*) to probe the expression of certain genes. LNA has further been used in fluorescence *in situ* hy-

bridization (FISH) experiments for fast detection at lower concentrations than native probes (*239*).

2.3   Carbocyclic nucleotide analogues

The vulnerability of the glycoside bond has inspired the synthesis of carbocyclic nucleic acids analogues where the ribose moiety in native nucleotides is replaced by a cyclopentane derivative. These compounds are generally speaking more resistant to nucleases and general acidic conditions, but less potent as antisense agents compared to the native sequences. Solved NMR (*240, 241*) and crystal structures (*242, 243*) of carbocyclic nucleotides incorporated into DNA have shown that the carbocyclic moiety does not disturb the global conformation, but take up very diverse conformations themselves, giving an insight of the inherent flexibility of this family of compounds.

2.4   Present work (Papers I-III)

The aim of our work in this field has been to further characterize and evaluate two chemically modified nucleoside building blocks, 2'-deoxyaristeromycin (Figure 9B) and 1-(1',3'-*O*-anhydro-β-D-psicofuranosyl)thymine (Figure 9C) for potential use in tuning the stability, preferred conformation and folding of oligonucleotides, as well as to learn more about the forces dictating the structure and dynamics of native oligonucleotides.
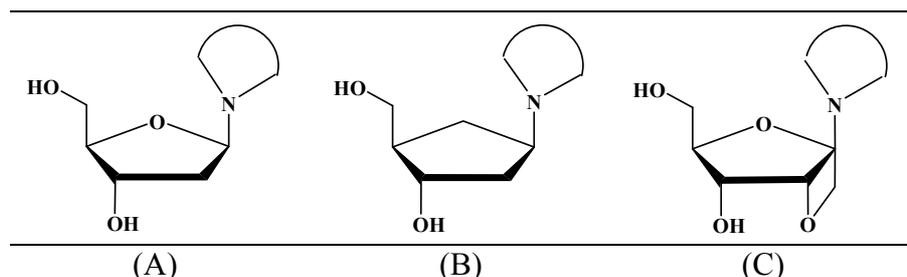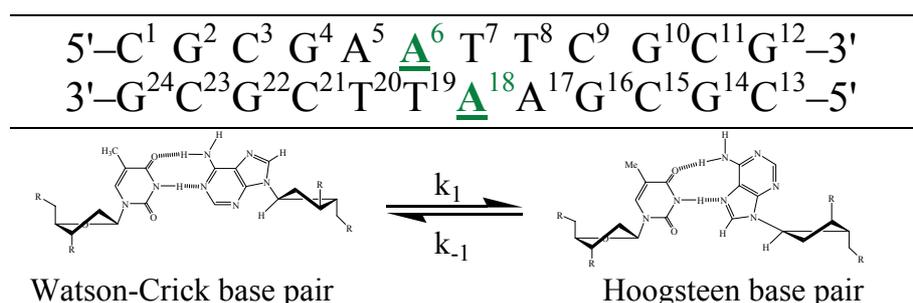

Figure 9. Schematic drawings of the modified ribose moieties (with attached side groups) of the nucleoside building blocks used studied in **Papers I** through **III**. (A) 2'-deoxyribo-, (B) 3'-hydroxy-cyclopentanylmethanol, (base = A, 2'-deoxyaristeromycin), (C) 1-(1',3'-*O*-anhydro-β-D-psicofuranose)-.

2.4.1   2'-deoxyaristeromycin (Paper I)

Aristeromycin was first discovered by Kusaka *et al.* to have antibiotic activity against *Xanthomonas oryzae* and *Pyricularia oryzae* (*244*). The 2'-deoxy and 3'-deoxy forms of the molecule have subsequently been analyzed in this laboratory by X-ray, NMR and *ab initio* calculations (*245*) to elucidate the impact of the absence of the O4'. The 2'-deoxy form of aristeromycin is completely devoid of *gauche* effects within the five-membered carbocyclic moiety replacing the deoxyribose unit of native DNA. The molecule is also devoid of the steric clash between the nucleobase and the O4' that is associated with the East barrier of pseudorotation. The average NMR coupling constants suggest that all forms of aristeromycin have a conformation in the East to Southeast region of the pseudorotation cycle. NOE difference experiments also suggested that the χ torsion exists in a quick ~1:1 equilibrium between *syn* and *anti* conformations.

In **Paper I**, the effect of the introduction of 2'-deoxyaristeromycin (Figure 9B) (**A**) in the A^6 position of the self-complementary Dickerson-Drew sequence (*111, 246, 247*) (Figure 10) was examined by NMR and computer assisted NMR constrained molecular modeling. Hoogsteen base pairing, which has previously only been observed in triplex (*37-42*) and tetraplex (*43-49*) structures, was for the first time directly observed in a duplex structure [although an old diffraction study observed that a general Hoogsteen model simulated the diffraction pattern of C(2) modified poly(A)·poly(U) duplexes better than the corresponding Watson-Crick- and reverse Hoogsteen models (*248*)]. The modified duplex was found to exist in two conformations, in a slow dynamic equilibrium. In the first conformation (~60% populated), all nucleobases are Watson-Crick base paired and display a structure that is isomorphic with the native Dickerson-Drew dodecamer. In the second conformation (~40% populated), the two central aristeromycins of the $\underline{A}^6 \cdot T^{19}$ and $T^7 \cdot \underline{A}^{18}$ base pairs are simultaneously flipped into *syn* conformation and engage in Hoogsteen base pairing with the opposite thymidines. The equilibrium constant, defined according to $K_{eq} = k_1/k_{-1}$ in Figure 10, is estimated to 0.58 and the thermodynamics of the transition between the two conformers are determined to the following values: k_1 (298K) = 3.9 ± 0.8 sec^{-1}; $\Delta H^{\circ\ddagger}$ = 164 ± 14 kJ/mol; $-T\Delta S^{\circ\ddagger}$ (298K) = -92 kJ/mol giving a $\Delta G^{\circ\ddagger}_{298}$ of 72 kJ/mol. E_a (k_1) = 167 ± 14 kJ/mol for the forward transition and k_{-1} (298K) = 7.0 ± 0.6 sec^{-1}, $\Delta H^{\circ\ddagger}$ = 153 ± 13 kJ/mol; $-T\Delta S^{\circ\ddagger}$ (298K) = -82 kJ/mol giving a $\Delta G^{\circ\ddagger}_{298}$ of 71 kJ/mol. E_a (k_{-1}) = 155 ± 13 kJ/mol

for the reverse transition. UV melting experiments determined the melting temperature of the modified duplex to be 2.4 ºC lower than the native dodecamer, which is a remarkably low destabilization considering the structural rearrangement that occurs in the modified system. This implies that the transition between Hoogsteen and Watson-Crick base pairs does not open up the duplex and let in much more water than normal base pair breathing does in the native duplex.

$$5'–C^1 \ G^2 \ C^3 \ G^4 \ A^5 \ \underline{\mathbf{A}}^6 \ T^7 \ T^8 \ C^9 \ G^{10}C^{11}G^{12}–3'$$
$$3'–G^{24}C^{23}G^{22}C^{21}T^{20}T^{19}\underline{\mathbf{A}}^{18}A^{17}G^{16}C^{15}G^{14}C^{13}–5'$$

| Watson-Crick base pair | Hoogsteen base pair |

Figure 10. The modified duplex exists in an equilibrium between a fully Watson-Crick base paired B-type duplex and a duplex where the two central 2'-deoxyaristeromycins of the $\underline{\mathbf{A}}^6{\cdot}T^{19}$ and $T^7{\cdot}\underline{\mathbf{A}}^{18}$ base pairs are simultaneously flipped into *syn* conformation and engaging in Hoogsteen base pairing with the opposite thymidines.

The structural impact of the two Hoogsteen base pairs was localized to the core of the helix. The global effect is only seen as a ~2-3 Å narrowing of the minor groove and a corresponding widening of the major groove (Figure 11). The two central base pairs are tilted and buckled, but otherwise reasonably planar. Only a few select backbone torsions were necessary to accommodate for the Hoogsteen base pair, mainly the α, δ and γ torsions of the core residues.

The East energy barrier of pseudorotation (Figure 4) consists of (1) the O4'-O3' *gauche* effect and (2) the steric bulk and electronegativity of the O4' (see section 1.5.1). The dramatic increase in polymorphism upon the substitution of the O4' for a CH_2 shows the importance of the stabilizing *gauche-* and steric effects involving the O4' in native DNA. The resulting flattening of the energy barrier of pseudo rotation through the O4'-*endo* conformation, making the sugar conformation as well as the correlated glycosyl torsion virtually free at room temperature. Under these conditions, the carbocyclic moiety will exist in any conformation that is stabilized by the surrounding structure elements.

Fully Watson-Crick base paired   Hoogsteen base paired core
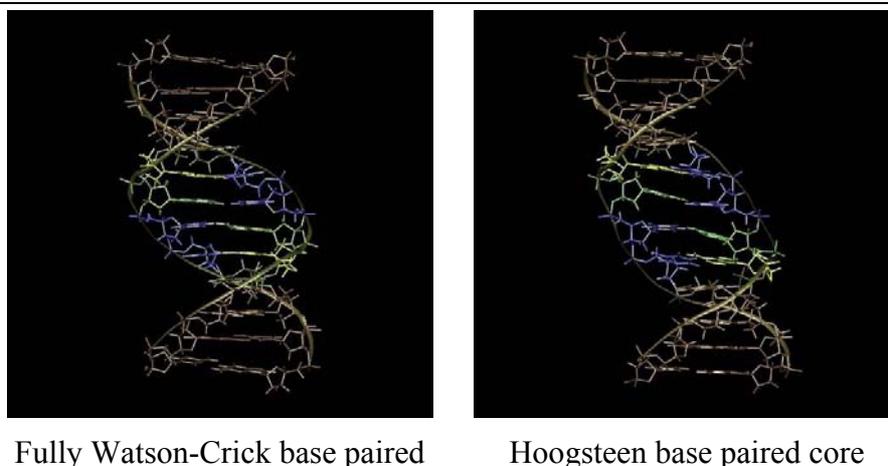
Figure 11. A side view into the major grooves of the two conformations of the 2'-deoxyaristeromycin modified Dickerson-Drew dodecamer. Key: 2'-deoxyaristeromycin (green), thymidine (blue) and 2'-deoxyadenosine (yellow).

In a contemporary study (*241*), a single 2'-deoxyaristeromycin substitution in an asymmetric undecamer sequence does not display any alteration of the conformation compared to the native sequence. The dramatic conformational polymorphism that is observed in our symmetric sequence implies that the close proximity of the two 2'-deoxyaristeromycins across the strands cooperatively makes it possible to stabilize the Hoogsteen base pairs. The fact that the bases always co-flip (*i.e.* there are no detectable populations of structures where one 2'-deoxyaristeromycins is Watson-Crick base paired and the other is Hoogsteen base paired) shows that the structural impact of one base taking up a *syn* conformation needs to be compensated for by the corresponding transition at the symmetric position in the opposite strand in order to form an energetically favorable structure in this sequence.

After the publication of **Paper I**, Hoogsteen base pairing has been discovered in single-crystal X-ray structures of the native d(ATA[Br]UAT) and d(ATATAT) sequences, which are found in the TATA box as well as regulatory regions of DNA (*249*). This discovery added more fuel to the question whether Hoogsteen duplex base pairing has any significance *in vivo*. In a recent publication, the X-ray structure of a DNA polymerase belonging to the Y family (human polymerase ι, hPolι) co-crystallized with a template primer and a replicative strand where the template adenosine forms a Hoogsteen base pair with the incoming 2'-deoxythymidine 5'-triphosphate (dTTP) has been solved (*250*). The remarkable feature of the hPolι compared to other polymerases is that it incorporates dTTP opposite a template adenosine

31

with at least several hundred-fold higher efficiency and fidelity compared to the reverse situation when the thymidine is in the template strand. The authors conclude that the Hoogsteen base pairing at the replicative end explains this feature and provides a mechanism for replication through minor-groove purine adducts that normally interfere with replication.

2.4.2   1-(1',3'-O-anhydro-β-D-psicofuranosyl)thymine (Paper II)

The influence of the conformationally restrained (3'-*endo*/4'-*exo*) nucleoside analogue, 1-(1',3'-*O*-anhydro-β-D-psicofuranosyl)thymine (*206, 251*) (**T**) on the thermodynamic stability of DNA·DNA and DNA·RNA duplexes as well as their abilities to show nuclease stability and to recruit RNase H for the down-regulation of target mRNA have previously been investigated in this laboratory (*202, 204, 205, 207, 208*). It is shown that a locked **T** protects five RNA residues downstream of the base pairing with the **T** from RNase H degradation. The thermal stabilities however decrease in *both* hetero- (DNA·RNA) and homo (DNA·DNA) duplexes by approximately 6 ºC per **T** modification when the modification is incorporated into the DNA strand**.**

  The structural effects of introducing the restrained residue in the Dickerson-Drew dodecamer (Figure 12) have been investigated by NMR and molecular dynamics (**Paper II**).

$$5'\text{--}C^1\ G^2\ C^3\ G^4\ A^5\ A^6\ \underline{\textbf{T}}^7\ \ T^8\ C^9\ G^{10}C^{11}G^{12}\text{--}3'$$
$$3'\text{--}G^{24}C^{23}G^{22}C^{21}T^{20}\underline{\textbf{T}}^{19}A^{18}A^{17}G^{16}C^{15}G^{14}C^{13}\text{--}5'$$
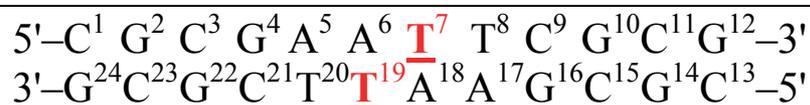
Figure 12. The sequence of the studied oligomer highlighting the position of 1-(1',3'-*O*-anhydro-β-D-psicofuranosyl) thymine modification.

  The DNA·DNA Dickerson-Drew dodecamer displays a drop in melting temperature, T_m, of approximately 10 ºC per $\underline{\textbf{T}}^7$ modification, to be compared to the ~6 ºC observed in the non-self complementary DNA·DNA and DNA·RNA sequences (*205, 207, 208*). This once more shows that two modifications close to each other in double-stranded DNA cause a larger perturbation than the sum of two isolated single modifications would have (compare with **Paper I**). It is also noteworthy that the dramatic drop in T_m is only seen when the modification is made on a pyrimidine nucleoside. DNA antisense strands including locked purines, **A** and **G**, form stable helixes with RNA

with melting temperatures very close to the corresponding native sequences (*206*).

Native duplex $\quad\quad\quad\quad$ $\underline{\mathbf{T}}^7$ Modified duplex

Figure 13. A side view into the major grooves of the two conformations of the native (left) and the modified (right) Dickerson-Drew dodecamer. Key: 1-(1',3'-*O*-anhydro-*β*-D-psicofuranosyl)thymine (green), thymidine (blue) and 2'-deoxyadenosine (yellow).

Despite the reduction of the T_m, all bases participate in Watson-Crick base pairing. However, the NMR constrained minimized structures and the MD trajectories expose the inability of the mod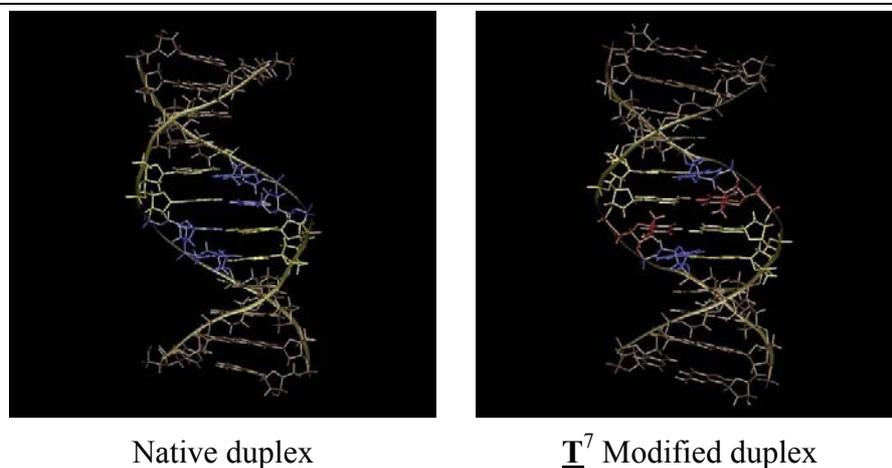ified duplex to maintain linear base pairs and base stacks at the $\underline{\mathbf{T}}^7{\cdot}A^6$ and $T^8{\cdot}A^5$ base pairs. The sugar moiety of the oxetane modified $\underline{\mathbf{T}}$ residue maintains its North conformation and A-type χ torsion, while all other residues retain their typical B-type conformations. The backbone torsion angles are strongly perturbed localized to the site of the oxetane $\underline{\mathbf{T}}$ incorporation. The β torsion is displaced from its normally preferred *ap* (*trans*) conformation to +*sc* (+*gauche*), balanced by a shift of the γ torsion from +*sc* (+*gauche*) to *ap* (*trans*). The α, ε, ζ and χ torsions are also shifted towards values associated with A-type conformation. The helical parameters changes are found to be mainly localized to the four central base pairs of the oxetane modified duplex. The central $\underline{\mathbf{T}}^7{\cdot}A^6$ and $A^6{\cdot}\underline{\mathbf{T}}^7$ base pairs are strongly staggered and stretched, resulting in non-linear hydrogen bonds. Further, there is a distinct roll of the base pair step between the two modified base pairs, $\underline{\mathbf{T}}^7{\cdot}A^6$ and $\underline{\mathbf{T}}^7{\cdot}A^6$ and there is an increased tilt (and slide) of the $\underline{\mathbf{T}}^7{\cdot}A^6/T^8{\cdot}A^5$ and $A^5{\cdot}T^8/A^6{\cdot}\underline{\mathbf{T}}^7$ base pair steps flanking the two modified base pairs. The

main effect on the global structure is 1 to 3 Å widening of the minor groove width (Figure 13).

Table 2. The rate constants of the imino protons of the native duplex and the $\underline{\textbf{T}}^7$ modified duplex exchange with the bulk water determined by the NOESY (**N**) two-proton buildup method (*252*) as well as the NOESY-ROESY (**N-R**) approach (*155*), as well as back-calculated from the T_1- (*14-18*) and line width differences, $\Delta\upsilon_{\frac{1}{2}}$ (*253*).

| | | | | k_{ex} (s^{-1}, 293 K) | | | | |
	Base pair	$(R_{1N}+k_{ex})$	$(R_{1N}+k_{ex})$	N	N-R	T_1^{-1}	ΔT_1^{-1} (II)-(I)	$\Delta\upsilon_{\frac{1}{2}}$ (II)-(I)
$\underline{\textbf{T}}^7$ modified duplex (II)	$\underline{\textbf{T}}^7$-A^6	45	26	5.0	47	11.5	11	15
	T^8-A^5	17	5.6	0.88	0.25	1.2	0.5	4.6
	C^9-G^4	18	4.7	2.3	0.0	0.71	0.0	0.6
	G^{10}-C^3	19	5.7	0.52	0.65	0.97	0.1	0.6
	C^{11}-G^2	33	15	3.4	7.1	5.3	4.0	5.2
Native duplex (I)	T^7-A^6	14	3.1	0.25	0.31	0.68		
	T^8-A^5	15	3.7	0.45	0.61	0.73		
	C^9-G^4	17	4.3	2.3	0.07	0.73		
	G^{10}-C^3	17	4.7	0.37	0.42	0.85		
	C^{11}-G^2	20	6.5	1.5	2.9	1.3		

The structural work has been expanded with a hydration study to elucidate if the distorted stacking causing the dramatic reduction in melting temperature per modification is due to water poisoning of the base pairs. It is found that the central modified base pairs exchange at least one order of magnitude faster with water than the corresponding base pair in the native duplex (Table 2), thus confirming that the reduction in melting temperature is due to a much stronger hydration of the helix core. The exchange rates (Table 2) together with the temperature profile of the **T**^{7} and T^8 aromatic protons (**Paper II**) shows that the structure melts simultaneously from the center, as well as from the ends of the duplex.

2.4.3 Charge transport in modified DNA (Paper III)

In related work (**Paper III**), the charge transfer through immobilized duplexes incorporating the locked 1-(1',3'-*O*-anhydro-β-D-psicofuranosyl)thymine building block, $\underline{\textbf{T}}$, (**Paper II**) has been studied by chronocoulometric analysis (stacking-mediated electrochemical reduction of methylene blue) (*254*). The method is sensitive to distortions in the stacking geometries and has previously been successfully

used to detect all single mismatches (*255*) and to monitor DNA-protein interactions (*256*).

When the modified **T** block is incorporated into one of the strands of a DNA·DNA duplex (Figure 14A), the stacking is perturbed in a way that is quantitatively very similar to the effect of a single mismatch (Figure 14B). However, when the same locked nucleotide is forming a DNA·RNA hetero duplex, the charge transfer remains undisturbed, as for the native DNA·DNA and DNA·RNA sequences (Figure 14C).
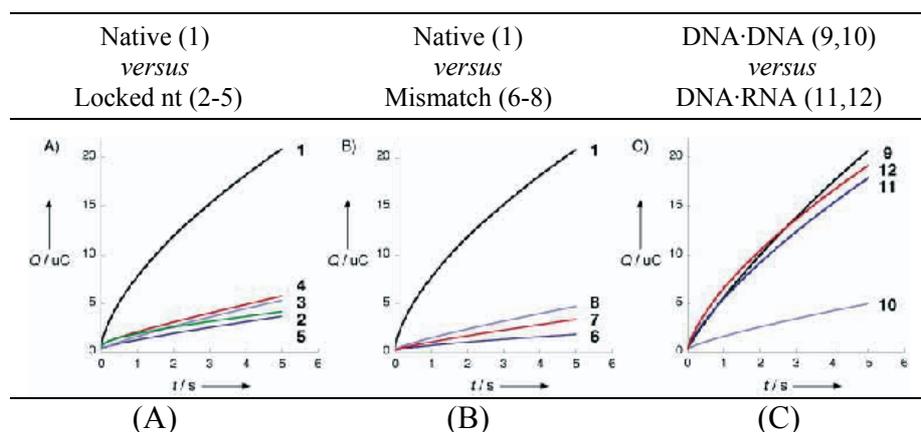
Native (1) *versus* Locked nt (2-5)	Native (1) *versus* Mismatch (6-8)	DNA·DNA (9,10) *versus* DNA·RNA (11,12)

(A)	(B)	(C)

Figure 14. (A) The charge transport of the modified building block incorporated in a DNA strand (2-5) is probed and compared with a native sequence (1). (B) The effect of the modification is also compared for a DNA homo duplex (native: 9, modified: 10) and DNA·RNA hybrid duplexes (native: 11, modified: 12). (C) For comparison, the native sequence (1) is also compared with three different point mismatches (6-8).

2.5 Conclusions

Perturbing native DNA by introducing chemically modified nucleotide analogues reveals intrinsic properties of the native system: The 2'-deoxy aristeromycin (**A**) structural study effectively displays how important the *gauche*- and steric effects of the O4' are for stabilizing the Watson-Crick helical structure in native DNA (**Paper I**). The cooperativity of the modifications is also highlighted. While a single modification has no structural impact (*241*), two adjacent symmetric modifications allow for the stable formation of Hoogsteen base pairs. When both the $\underline{A}^5$ and $\underline{A}^6$ positions in the same sequence are simultaneously modified, four or more different substructures exit in slow equilibrium (unpublished work).

In contrast, the locked **T** modification in **Paper II** shows how important it is for the sugar moiety to maintain a certain degree of flexibility. The introduction of rigid A-type conformation nucleotide into a helix that otherwise preferentially takes up a B-type conformation significantly disturbs the stacking, dehydrates and destabilizes the helix. Even though the amplitude of the structural change is much larger in **Paper I**, the helix complex is not as destabilized as the helix in **Paper II**. This is most likely because the flexibility of the **A** allows the helix to maintain a sufficiently good stacking to keep the water extruded from the core of the duplex. The locked nature of the **T** residue however transfers to the nucleobase, restricting the available stacking geometries, making it unable to form linear hydrogen bonds without disturbing the stacking geometry and causing strain in the sugar-phosphate backbone.

3 Single-stranded oligonucleotides

Nucleic acids need to go through the unpaired, single-stranded form during many of the central biological processes, like mRNA processing and translation. Therefore, the properties of single-stranded nucleic acids are interesting in general, and the differences between ssDNA and ssRNA in particular, as their functions *in vivo* are completely different.

3.1 *Pre-organization of single-strands*

The intra-strand stacking interactions of single-stranded DNA and RNA have been quantified by UV spectroscopy (*257*), differential scanning calorimetry (DSC) (*258-260*), circular dichroism (CD) (*261, 262*), optical rotatory dispersion (ORD) (*262-264*) and sedimentation/viscosity (*265, 266*), vapor pressure osmometry (*267*) and low-field NMR (*267-272*) in 0-2 M NaCl. Most of the studied nucleobases are significantly preorganized in stacked conformations. Some trends are identified: The salt dependence and cooperativity of single-strand stacking is negligible, but the nucleobase sequence is very important. The stacking capability of uridine is very poor - there is no confirmed preorganization in neither UpU (*257*) nor poly(U) (*265, 266*), and uridine bases are sometimes flipped out from an otherwise stacked sequence, interrupted by an uridine (*271, 272*). However, these results are in contradiction with the fact that a 3' dangling uridine provides somewhat more stability to a duplex structure than a dangling cytidine on the same core sequence (**Paper VI**) (*273-278*), which means that the uridine can stack well on a blunt end. A possible explanation is that the different dipole moments and electronic configurations of uridine and cytidine (Figure 2) give them different optimal stacking geometries, which in turn gives them different preferences for stacking with the same strand, with the opposite strand, or with the sigma framework making up the hydrogen bonds of a neighboring base pair through offset stacking (Figure 3).

  The experimental studies on the internal single-stranded interactions have also been supported by theoretical studies of stacking in water (*279, 280*) on the MP2/6-31* level. The electrostatic term is found unfavorable for stacking, and both these studies support the conclusion that nucleobase stacking is driven by solvent effects and van der

Waals interactions rather than favorable electrostatics (*72, 73*). The electrostatics can however still be a very important factor in determining the stacking geometry by steering it to the conformation that has the weakest repulsions.

The contribution to duplex stability coming from single-strand pre-organization has been studied by Vesnaver and Breslauer by comparing the enthalpies of melting by UV spectroscopy/DSC with the enthalpy of duplex formation by isothermal batch-mixing calorimetry (*258*). It is found that approximately one third of the free enthalpy (ΔH^o_{ds} [UV/DSC] = 117.0 kcal/mol, ΔH^o_{ss1} [UV/DSC] = 29.1 kcal/mol, ΔH^o_{ss2} [UV/DSC] = 27.1 kcal/mol, $\Delta H^o_{ds, 298K}$ [isothermal batch-mixing calorimetry] = -56.4 kcal/mol) of stabilization of the d(CGCATGAGTACGC)·d(GCGTATCATGCG) duplex structure at 25 ºC is provided by single-strand preorganization, even though the individual single-strands are only marginally stable since their enthalpies and entropies are relatively well balanced at this temperature. Thus, it is well established that single-stranded nucleic acids have a high degree of preorganization at low temperatures. However, high field NMR has, to the best of my knowledge, neither been used to characterize the pre-organization nor to pinpoint any different preferences in stacking geometries for unbound ssDNA and ssRNA.

3.2 pK$_a$ modulation in nucleic acids

The catalytic ability of RNA was first discovered in self-splicing RNA (*181*), followed by the discovery that the tRNA precursors are catalyzed by the RNA component of RNase P (*182*). This was surprising since nucleic acids lack the functional groups that are successfully deployed by protein enzymes: the imidazole of Histidine, the carboxylate of Aspartate and Glutamate, the alkyl amine of Lysine and the sulfhydryl of Cysteine (*281*). The catalysis of the phosphotransesterification and hydrolysis reactions involves the donation of a proton from the attacking group and the acceptance of a proton of the leaving oxygen group. Protein enzymes often accomplish this by a general acid-base catalysis reaction, using functional side chains with a pK_a close to neutral to activate the attacking and leaving groups, as this allows for the highest concentration of strong acid or base to exist in its active protonated/deprotonated form. Lacking the natural functional groups with pK_a's close to neutrality, nucleic acids can fill the requirements for efficient catalysis in two ways. Either by stabilizing the attacking and leaving groups by aligning a metal ion, or by modu-

lating the pK_a of primarily Adenine and Cytidine closer to neutrality (*282*), thereby increasing their efficiency as general acids/bases.

Even though it has been proposed that nucleic acids are unlikely to act as efficient acid-base catalysts, more recent studies have shed new light on the subject. The pK_a values of nucleobases in biologically relevant nucleic acids and nucleic acids/protein complexes can be significantly modulated (*283-295*) through interactions with its immediate surroundings compared to the corresponding nucleoside, directly increasing their performance as acid-base catalysts in ribozymes (*285, 290, 291, 295, 296*) and leadzymes (*283, 284*), and as substrates to for example DNA glycosylases (*288, 289*). The pK_a of nucleobases in an active site can be modulated by (1) hydrogen bonding in wobble base pairs (*283-285, 293, 294*), (2) salt bridge formation (*284*) or (3) specific folding, creating a unique local electrostatic environment or a hydrophobic pocket around the active site (*282*) through stacking interactions.

Thus, the apparent pK_a of an exchangeable proton on a nucleobase carries information about the charge distribution in the base as a function of its interactions with the surrounding electron systems, as well as the accessibility and dielectric constant of the surrounding media.

3.3 *Present work (Papers IV and V)*

The present work on single-strands is the continuation of thorough pK_a studies previously performed in this laboratory by Acharya *et al.* (*297-301*).

3.3.1 *Sequence dependence of pKa perturbation (Paper IV)*

Previous work on single-stranded nucleic acids in this laboratory has showed sequence dependent modulation of the apparent pK_a of dinucleotides (*301*), trinucleotides (*298*) and short oligomers (*297*). It is however difficult to draw any final conclusions on the effects of stacking on the pK_a modulation from the studies on short sequences, as these structures reside more in a random coil conformation. Therefore, these studies have been expanded by a comparative study of ssDNA and ssRNA heptamers of the sequences: 5'-CAQ^{1}GQ^{2}AC-3', where Q^1 and Q^2 are either A or C in the four possible combinations of ssDNA and ssRNA, resulting in a total of 8 heptamers (**Paper IV**). The ΔpK_a

of the guaninyl of the investigated trimers display a pK_a modulation in the $0 < \Delta pK_a < 0.7$ range (*298*), while the heptamers display a modulation in the $0.5 < \Delta pK_a < 1.5$ range (**Paper IV**). Thus, the nucleobase dynamics directly affects the efficiency of the stacking interactions, and hence, how well the potential of the nearest neighbor effects are utilized.

  The pH titration of the imino proton of guanosine, incorporated in different heptamer sequences, in **Paper IV** shows that single-stranded nucleic acids are capable of modulating the apparent pK_a of a guanosine by as much as 1.5 units, without advanced folding into higher ordered structures. A direct correlation is found between the amount of stacking, reflected by the relative shielding of the H8 proton of the guanine, and the ΔpK_a (Figure 15).
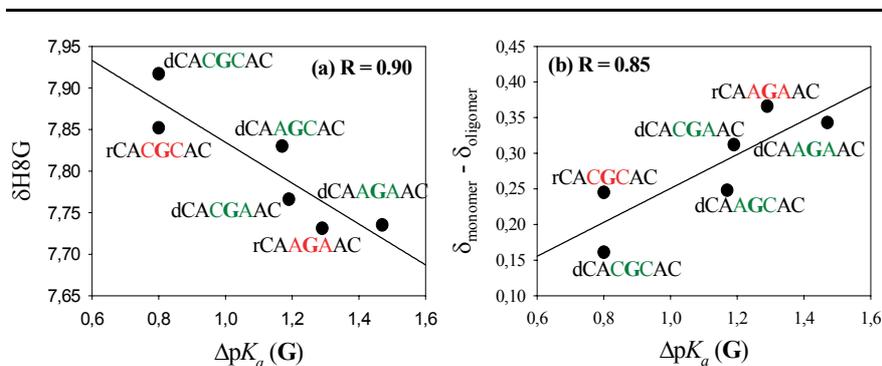

Figure 15. Plot of the ΔpK_a of the guaninyl imino proton *versus* (a) the chemical shift of the H8**G** proton, R = 0.90 and (b) the oligomerization shift of the H8**G** proton, R = 0.85, respectively. The central trio made up by the guanosine (**bold**) and its neighbors is highlighted in green for DNA and red for RNA.

3.3.2 *Stacking patterns of ssDNA and ssRNA (Paper V)*

  Differences in the NOESY cross peak intensity patterns are observed for ssDNA and ssRNA in **Paper V**. The intra-residue H6/H8-H3' and the inter-residue H6/H8$_{(n)}$-H3'$_{(n-1)}$ distances are particularly sensitive to the populations of A-type *versus* B-type conformations. Significantly stronger cross peaks involving the 3' protons were indeed observed for the ssRNA compared to the ssDNA, showing that ssRNA spends more time A-type conformation than ssDNA and *vice versa* (Table 3). MD trajectories of the single-stranded DNA and RNA were simulated in explicit water for 1.5 ns, using the estimated nOe intensi-

ties as loose distance constraints. The resulting average structures graphically revealed distinct directional differences in the stacking geometries of each dinucleotide step between ssDNA and ssRNA (Figure 16). The relatively electron-rich (Figure 2) imidazole stacks above the relatively electron-deficient pyrimidine (5'→3') in ssDNA, while, on the contrary, the pyrimidine stacks above the imidazole (5'→3') in ssRNA.

Table 3. Experimental NOESY cross peak data compared with the corresponding expected distances (Å) measured in models of the single strand of the canonical A-, B- and Z- forms of DNA and RNA. The observed cross peaks have been categorized as strong, medium or weak cross peaks. Strong peaks are drawn in **bold**.

	canonical distance (Å)			nOe intensity	
Distance	**B-type**	**A-type**	**Z-type**	**ssDNA**	**ssRNA**
H6/H8-H3'	4.4	**3.2**	5.1	M	S
H2-H2'/"	7.0/5.8	4.6/5.4	5.8/4.6	-/W	M/#
H5-H3'	6.4	4.9	7.0	W	M
H6/H8-H1' $_{(n-1)}$	**3.0**	**4.3**	7.0	**S**	S
H6/H8-H3' $_{(n-1)}$	5.1	**3.2**	6.9	M	S
H5-H1' $_{(n-1)}$	3.8	5.0	5.2	M	W
H5-H3' $_{(n-1)}$	5.5	3.7	4.4	W	M
H2-H1' $_{(n+1)}$	4.6	**3.5**	5.2	M	S
H2- H2'/" $_{(n+1)}$	6.8/6.2	5.3/6.2	10.4/11.7	-/-	W/#
H2-H4' $_{(n+1)}$	5.7	6.3	6.8	W	-

- – not detectable; W – weak; M – medium; S – strong
- RNA is devoid of H2"

ssDNA	ssRNA
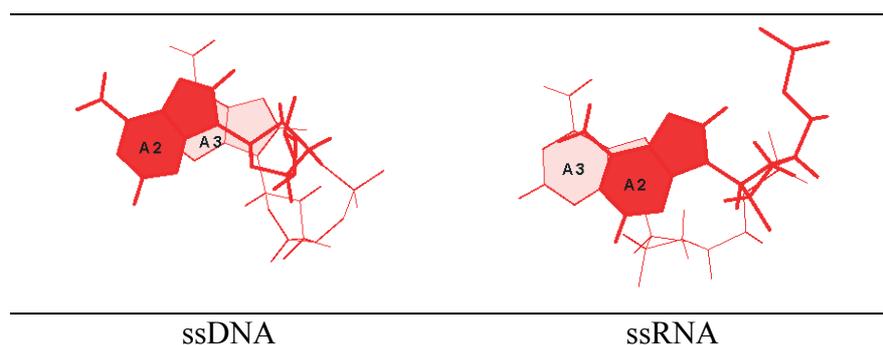
Figure 16. The stacking geometry at the A^2-A^3 dinucleotide steps of the minimized average structures of the last 100 ps of the 1.5 ns MD simulations of the d/r(G^{1}A^{2}A^{3}A^{4}A^{5}C^6) sequences.

This conformation likely minimizes the repulsion between the π−π surfaces of the two bases, and simultaneously positions the partially positive σ-frame protons directly perpendicular over the π surface of the neighboring base, much like in the stair motifs that are commonly seen in nucleic acids-protein interactions (*302*).

In order to verify the found stacking patterns against the raw data, screening values of each H2 and H6/H8 marker proton in the oligomer was calculated (**Paper V**) and compared with the oligomerization shift (*i.e.* $\delta_{monomer}$-$\delta_{oligomer}$) of each proton (Figure 17). The relatively good correlation of R = 0.83 for all protons validates the observed stacking patterns in the ssDNA and ssRNA simulations. The correlation disappears completely (R = 0.077) when the oligomerization shifts of the ssRNA and ssDNA structures are inverted, confirming that there really is a significant difference between the stacking patterns of the two hexamers.
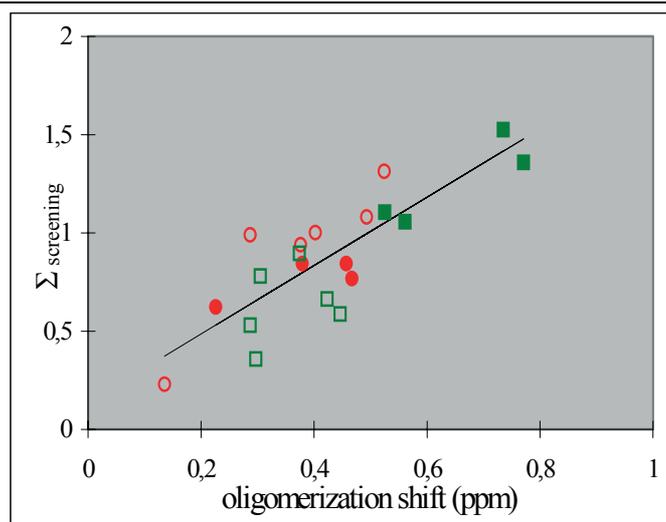
Figure 17. Correlation plot (R = 0.83) between the oligomerization shift (Δδ) *versus* the combined effect[*] of the neighboring bases for the modeled ssDNA (■: H2, □: H6/H8) and ssRNA (●: H2, ○: H6/H8).

* The displacement in the X-Y plane of each proton (H8, H2 and H6) from the nearest edge of the neighboring nucleobase was measured in both 3' and 5' directions. The distances were then normalized to a sigmoidal, $y = 1-1/(1+10^{(2-x)/2})$, and summed to give a value that is proportional to the screening received from the neighboring ring systems.

3.3.3 pKa-structure correlation (unpublished data)

Since the single-strand stacking geometries are correlated with the chemical shifts of the nucleobase protons (**Paper V**) and the chemical shifts are in turn correlated with the ΔpK_a of the nucleobase (**Paper IV**), a direct correlation between stacking geometry and ΔpK_a is likely to exist. In a preliminary experiment, the screening coefficient was roughly estimated for the imino proton of guanosine in 14 different sequences, extrapolated from the stacking patterns found in **Paper V** for ssDNA and ssRNA respectively. It was found that the more buried the imino proton is, reflected in a higher screening value, the higher its pK_a becomes (Figure 18), R = 0.88.
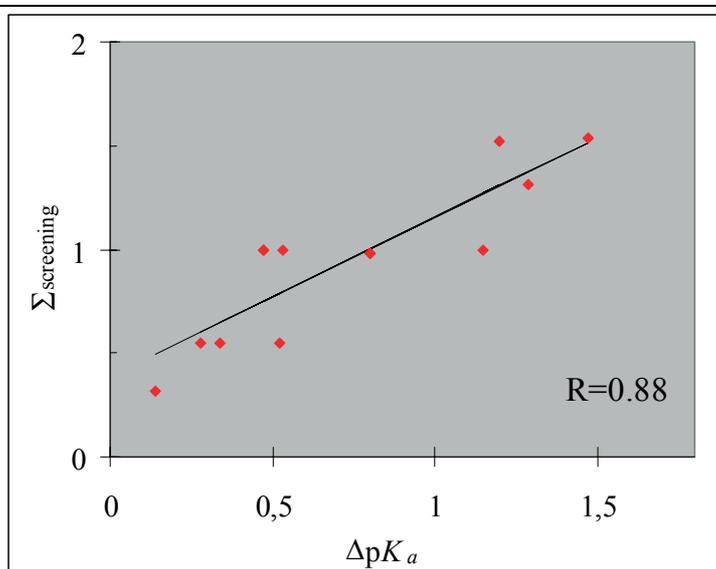
Figure 18. The screening factor of the imino proton of **G** calculated using the stacking pattern for d**G**AAAAC and r**G**AAAAC plotted versus the pK_a of the following compounds: d**G**AAC, d**G**AAAC, d**G**AAAAC, dCAA**G**AAC, dCAA**G**CAC, dCAC**G**AAC, dCAC**G**CAC, dCAA**G**, r**G**AAC, r**G**AAAC, r**G**AAAAC, rCAA**G**AAC, rCAC**G**CAC, rCAA**G**. A correlation factor of R = 0.88 is found by linear regression.

This effectively shows that the physico-chemical properties of the nucleobases, in this case reflected by its pK_a, are directly influenced by the stacking interactions with the neighboring bases in single-stranded nucleic acids, in a way that reminds of face-selective conformation controlled reactions (*303-305*) used in synthetic chemistry. This also provides a possible geometrical explanation as to why for

example the pK_a of the guanosine imino proton is 9.76 in rGAAC, while it is 9.46 in the rCAAG sequence (*297*), even though the latter is predicted to have a higher pK_a because it has a 5' phosphate, which is known to raise the pK_a of monomeric guanosine from 9.25 to 9.74 for 5'-GMP.

  Even though it is clear that the amount of stacking at the exchangeable proton protects it from the bulk water, it is not possible to conclude if this is a direct electronic effect on the proton itself, increasing its electron density and thereby making it harder to extract from the nucleobase, or if it is a geometric/electrostatic effect, making it less probable for an anion to approach the buried proton by Brownian motion, both because of steric shielding and because of a possible charge-repulsion between an approaching anion and the π-surface of the neighboring nucleobase.

3.4   Conclusions

The pK_a titrations (*297*) (**Paper IV**), together with the found differences in stacking geometry between ssDNA and ssRNA (**Paper V**), have highlighted how the pre-organization of the stacking geometries of single-stranded nucleic acids have a direct influence on their different physicochemical properties. (1) The amount of pre-organization has a direct influence on the stability on any interactions formed with the oligonucleotide. The higher the degree of pre-organization, the lower the entropy penalty that has to be paid upon formation of higher ordered structures due to the freezing out of conformational freedom. (2) The modulation of the apparent pK_a of nucleobases, depending on the local geometry, and hence the chemical environment around it, can be tailored to facilitate catalytic activity. (3) The directional differences in single-strand pre-organization between ssDNA and ssRNA can be used to understand the stability of higher ordered structural motifs. One example of this is the dangling end phenomenon which is discussed in Chapter 4. The found stacking geometries could possibly also be used to understand more about the stability of some mismatches, bulges and loops in DNA and RNA. In the extension, any insights that can lead to a higher understanding of the mechanisms behind stability, folding and reactivity of nucleic acids and their derivates are important for the development of nucleic acid analogues into therapeutic agents or biomolecular tools.

4   Dangling ends

A dangling end is an unpaired residue that is attached to either end of a double helix structure (Figure 19). These overhangs are found in native systems like the acceptor stem of tRNA, which has a NCCA nucleobase overhang that is essential for its function and stability (*306-308*). Dangling ends also play stabilizing roles in the interactions between the mRNA and the ribosome in protein synthesis (*309, 310*) and between small interfering RNA (siRNA) and mRNA in RNA interference (*311-314*). The addition of a native dangling end can increase the stability of the core duplex by almost 2 kcal per mol, even though it does not participate directly in any hydrogen bonding with the opposite strand.
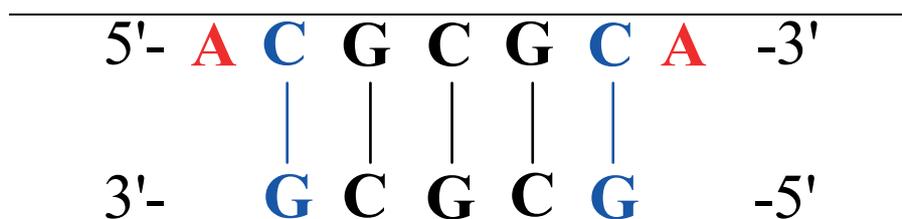

Figure 19. Schematic representation of a sequence with 5'- and 3'-*dangling-end* adenosines (**red**) over C-G *closing base pairs* (**blue**) attached to the G-C-G core duplex (**black**).

4.1   *Thermodynamic stabilization of dangling ends*

Martin *et al.* (*315, 316*) first identified the dangling-end phenomenon in partially self-complimentary RNA. The stabilization potentials of dangling ends have since then been thoroughly and systematically mapped by melting studies on short core duplexes of varying sequence and dangling base by NMR (*317, 318*) and UV spectroscopy (*273-278, 319*).

  The most striking feature of dangling ends is that there is a pronounced difference in the stabilization potential depending on whether you attach it to the 3'- or the 5'-end of a helix, and whether you attach it to a DNA- (*319*) or RNA (*275*) core duplex (Table 4). In RNA, the 3'-end has a significantly higher stability potential (-1.8 kcal/mol) compared to the 5'-end (-0.5 kcal/mol). The situation is less pronounced in the more flexible and polymorphic DNA, where the two

ends have a similar stabilization potential - the 5'-end (-1.0 kcal/mol) being slightly favored over the 3'-end (-0.9 kcal/mol). Thus, there is a directional preference in the interactions of the unpaired (*i.e.* single-stranded) dangling residue, which is similar to the directional differences in stacking patterns presented in **Paper V**.

Table 4. Summary of the thermodynamic gain upon dangling end attachment to DNA (*319*) and RNA (*275*) core duplexes of all different dangling end/closing base pair combinations.

	RNA		DNA	
	$-\Delta\Delta G_{37}^0$ (kcal/mol)	average	$-\Delta\Delta G_{37}^0$ (kcal/mol)	average
3'	**0.1 – 1.8**	**0.8**	-0.3 – 0.9	0.3
5'	0.0 – 0.5	0.2	**-0.5 – 1.0**	**0.4**

4.1.1 Dangling ends on RNA duplexes

A comparison of the stabilities provided by different combinations of dangling ends and closing base pairs at the 3'-end in the thermodynamic library established by Turner *et al.* (*273-278*) provides some insight into which factors determine dangling end stabilization. (i) The size of the dangling nucleobase is of primary importance. A purine always provides more stabilization (approximately -0.5 kcal/mol) than a pyrimidine in the same position. (ii) The purine/pyrimidines sequence of the overhang also plays an important role. More efficient stabilization is always achieved if the dangling base is larger than the base it stacks upon. A purine (*R*) stacking on a pyrimidine (*Y*) provides 1.5-1.8 kcal/mol, followed by equally sized bases that provide a stabilization of ~1.1 kcal/mol. A pyrimidine base stacking over a purine base always provides less than 0.6 kcal/mol. The sequence dependency of the stability can be written as follows: $\frac{5'-YR-3'}{3'-R--5'} > \frac{5'-RR-3'}{3'-Y--5'} =$

$\frac{5'-YY-3'}{3'-R--5'} > \frac{5'-RY-3'}{3'-Y--5'}$. (iii) The number of hydrogen bonds of the closing

base pair directly affects the potential stabilization of dangling end attachment. The maximum stabilization over a G·C base pair is 1.8 kcal/mol, while an A·U base pair is never stabilized by more than 0.7 kcal/mol.

46

4.1.2 Dangling ends on DNA duplexes

The effects of dangling ends are weaker and less predictable in DNA (*319*). There is a small preference for stabilization at the 5'-end over the 3'-end, but the difference is small and exceptions to the clear trends observed in RNA exist. The increased flexibility in DNA compared to RNA most likely makes the size and shape of the dangling end less dominant, as DNA is more prone to rearrange. For the same reason, the dynamics of dangling DNA bases are less restricted and therefore shield the closing base pair less efficiently.

4.1.3 Dynamics of the dangling residue

Further UV melting studies have shown that the dangling end stabilization increases for every additional dangling base that is attached, up to four bases of poly-A: $\Delta\Delta G^{\circ}$ of $\frac{5'-CA-3'}{3'-G--5'}$ = -1.5 kcal/mol and $\Delta\Delta G^{\circ}$ of

$\frac{5'-CAAAA-3'}{3'-G----5'}$ = -2.5 kcal/mol (*320*). This implies that the efficiency of the

dangling end effect is enhanced by the cooperative stacking of the poly-A tail, making the innermost A spend more time in a stacked conformation than the outer ones. Similarly, studies on chemically modified dangling residues (*321-327*) have shown that modifications that disfavour destacking or strengthens the stacking interaction of the dangling residue (increased polarizability (*322*), hydrophobicity (*327*) and methylation site and ion substituent (*324*)) leads to an increased dangling end effect. It has also been shown that by appropriate attachment of fused multi-ring systems [4-desmethylwyosine (*324*), quinolones (*323*), phenazinium (*20, 328*), pyrene and phenanthrene (*327*), phenylurea and naphtylurea (*326*), cholic acid (*329, 330*) and a 5'-acylamido oligonucleotide library (*331*)] to both DNA and RNA duplexes can stabilize them by as much as 4.5 kcal/mol. This is most likely a combination of favourable dynamics and a large shielding area.

4.2 *Present work (Paper VI)*

The directional differences in stacking pattern between ssDNA and ssRNA identified in **Paper V** provide a possible source for the directional differences reported in dangling end stabilization (*273-278, 319*). The stabilization trends identified above, together with the ear-

lier observation that the imino proton is protected from exchange with the bulk water in tethered duplexes (*20, 157, 328, 332, 333*), inspired an attempt to correlate the stacking geometries of dangling ends with the thermodynamic stabilization they provide through a data mining study.

4.2.1 *Dangling end stabilization-geometry correlation*

In **Paper VI**, the stacking geometries of dangling base motifs in 105 crystal/NMR structures containing single-strand to double-strand transitions have been studied. Qualitatively, the directionality in stacking pattern described in **Paper V** is commonly observed for the unpaired dangling residue relative to the neighboring base in the extracted DNA and RNA X-ray and NMR structures. A screening value for each of the extracted dangling end geometries was calculated from the sum of the relative displacements of each atom participating in hydrogen bonding relative to the dangling base, thus quantifying how well the hydrogen bonds are buried below the dangling end.
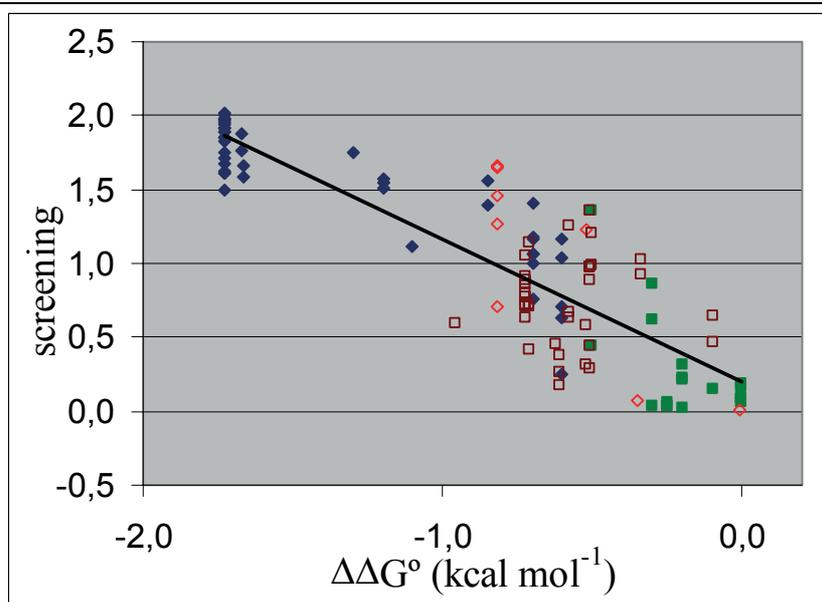
Figure 20. Correlation plots of the hydrogen bond screening versus the thermodynamic stabilization ($\Delta\Delta G^{\circ}_{37}$). The data points from both 3' RNA (◆), 5' RNA (■), 3' DNA (◇) and 5' DNA (□) dangling-ends fall on the correlation line and gives a correlation factor, $R = 0.873$. Considering only the points from RNA gives a better correlation, $R = 0.934$, showing that dangling-ends on RNA are more ordered than dangling-ends on DNA, $R = 0.376$.

It is found that this screening value is directly correlated to the thermodynamic stabilization that is provided by the corresponding dangling end sequence (Figure 20) collected from the literature (*273-278, 319*). The direct correlation of the dangling end stability with how well the atoms participating in the hydrogen bonds of the closing base pair are buried made us conclude that the increased stability of dangling end attachment is the effect of the dangling end effectively restricting the access of the bulk water and ions to the hydrogen bonds of the closing base pair (*21*). The result is a reduction of the dielectric constant of the microenvironment experienced by the hydrogen bonds, thereby increasing their strength (*57, 58*). In other words, the hydrogen bonds are protected from the solvent so that the donors and acceptors of the closing base pair do not have to compete with the surrounding water molecules for hydrogen bond formation.

Internal base pairs are known to be more stable than the corresponding terminal base pairs (*334-342*) from nucleic acids stability prediction algorithms. The dangling end gives the terminal base pair a character that is more like an internal base pair by screening it from the bulk solvent much like a neighboring base pair otherwise would. Thus, the dominating stabilizing contribution from attaching a native dangling end residue is not a direct interaction with the opposite strand, but rather a modulation of an already present interaction - the terminal hydrogen bonds.

In addition to the geometric influence shown in the correlation above, the stabilization is tuned by the dynamics of the dangling residue. We conclude that it is the absence of the O2' effects in DNA compared to RNA gives a DNA dangling base more geometrical freedom (*Section 1.5.1*). This makes it much more complicated to predict the geometry of DNA dangling end from the sequence only as they are more likely to be strongly affected by crystal packing forces upon crystallization. The increased flexibility of DNA can also have a positive effect on the stacking geometry as it can reach conformations unavailable to the corresponding RNA. For example, dangling end screening at the 3' end of DNA is often greater than the prediction from the stacking patterns in **Paper V**. However, the increased motional freedom of the deoxyribose linker compared to the ribose linker makes it necessary to freeze out more degrees of freedom and therefore the lifetime of the stacked state over the destacked state is reduced in DNA, reducing the stabilization potential of DNA dangling ends.

4.3   Conclusions

It is known that the strength of hydrogen bonding is proportional to the dielectric constant of the solvent (*57, 58*). The above correlation (**Paper VI**) shows how the strength of each individual hydrogen bond at the terminus of a duplex can be directly modulated by restricting the accessibility of water molecules and ions that compete for the hydrogen bond donors and acceptors of the terminal base pair. Similar drops in stability accompanied by increased exchange rates with water have been observed for various mismatches (*162, 321, 337, 338, 340, 343-345*). This highlights how the stacking ability (the protection against water poisoning of the hydrogen bonds) directly modulates how efficiently the potential of the base pairing interaction is utilized, not only at the terminus, but in the entire helix. The hydrogen bonding, in turn, stabilizes the stacked conformer of the nucleobases, which is evident from the fact that the nucleobases spend more time in a stacked conformation in a double-strand than in the corresponding single-strand (**Paper V**). The favorable enthalpy of the hydrogen bond interactions helps to pay for the loss of entropy associated with the freezing out motional freedom when going from random coil to a stacked structure. Thus, the stacking and hydrogen bonding in nucleic acids stabilize each other in a synergetic manner.

4.4   Discussion

Under this paragraph I take the liberty to speculate more freely around the dangling end observations and their possible implications.

Nature has tuned the geometries of the nucleic acids bases in such a way that the C1'-C1' distances and symmetry of C·G, G·C, A·T/U and T/U·A base pairs are near identical (*4*). This has the effect that the helix can maintain a well stacked, and hence dehydrated, structure independent of its sequence. The sequence context can affect the helical conformation of the duplex, but both the A-, B- and Z-type conformations have the common feature that they all stack very efficiently. Therefore, as long as there are no mismatched bases, the hydrogen bonds in the core of nucleic acids duplexes are dehydrated (*21*), enabling strong hydrogen bonding. While hydrogen bonding and nucleobase stacking cooperatively stabilize a matched base pair, both the hydrogen bonding- and stacking critera are very unlikely to be simultaneously satisfied in a mismatched native sequence. The loss of synergy between hydrogen bonding and stacking can provide an extra steep energy profile between a matched and a mismatched sequence,

thereby helping nature to maintain its high specificity in nucleic acids recognition. The situation is more complex in the replication, transcription and translation of nucleic acids. The fact that non-polar size complementary synthetic nucleosides can function well with DNA polymerases, both as template and as incoming triphosphate, suggests that steric exclusion and electrostatic repulsions in the tight active site are the most important factors for maintaining high fidelity replication [reviewed by Kool (*346*)].

On a side note, the stability of a double-stranded structure has often been described as the sum of the contributions from hydrogen bonding, stacking and phosphate repulsions, modulated by solvent- (dielectric constant, counter-ions) and thermodynamic effects (entropy of internal motions and solvent molecules). Even though the stability is described as a sum, the interdependency between them has the effect that they are not linearly additive. In particular, the synergy between the stacking and hydrogen bonding interactions discussed above highlights the complexity of the nucleic acid stability and how difficult it is to quantify the relative contributions from each of these interactions to the total stability of a double strand.

5 Acknowledgements

6 Sammanfattning

Avhandlingen sammanfattar resultaten av mina studier på de molekyler som utgör vårt arvsanlag, DNA och RNA. De grundläggnade resultaten är framtagna med hjälp av en spektroskopisk metod (NMR, Kärnmagnetisk resonans) som bygger på de energinivåer som uppstår när magnetiskt aktiva atomkärnor placeras i ett starkt magnetfält. Med hjälp av denna metod kan man bestämma avståndet mellan alla olika väteatomer i en molekyl, eller andra dynamiska egenskaper som beror av temperatur eller koncentration i provet. Med hjälp av de egenskaper som man bestämmer experimentellt kan man sedan skapa datorsimulerade strukturer och anpassa dessa så att de överensstämmer med experimenten. På detta sätt kan man med hjälp av NMR bestämma strukturen på korta sekvenser av DNA och RNA eller medelstora proteiner.

I min första publikation undersöker jag vilken effekt det får på en tolv nukleotider lång DNA-sekvens att byta ut en syreatom i en av dessa nukleotider mot ett kolväte. Resultatet visar att strukturen blir mer flexibel och att det uppstår en långsam jämvikt mellan den naturliga DNA-formen och en ny typ av basparning som inte tidigare studerats i detalj i dubbelsträngat DNA där den ena sidobasen roterat runt sin egen axel och istället låter den andra sidan av sig baspara med sin partner. På senare tid har man sedan upptäckt att denna typ av basparning kan förekomma i viss mån vid kopieringen av våra arvsanlag i våra celler.

Det andra projektet är en strukturbestämning av samma DNA-sekvens där jag bytt ut en annan nukleotid mot en variant som är låst i en form som normalt är vanlig i RNA och därför inte stämmer överens med de andra nukleotiderna i DNA sekvensen. Studien undersöker vilken effekt förändringen har på strukturen som helhet och dess stabilitet. Resultaten visar att dubbelsträngen blir starkt försvagad runt om modifikationen och att dubbelsträngen smälter både från ändarna och ifrån mitten när temperaturen höjs. Ett relaterat arbete visar också att transporten av laddning genom samma molekyl går betydligt långsammare som en direkt effekt av destabiliseringen. Karaktäriseringen av låsta- eller på annat sätt förändrade nukleotider är viktigt för att utvidga vår kunskap om konstgjorda byggdelar som i förlängningen kan användas för att rikta läkemedel direkt mot gener som orsakar sjukdomar.

De övriga studierna har fokuserat på enkelsträngat DNA och RNA och dess egenskaper. Enkelsträngade varianter av dessa molekyler förekommer i flera stadier av cellens naturliga liv och är helt nödvändiga för dess funktion. En ökad förståelse av dessa former kan ytterligare hjälpa oss att förstå hur vi fungerar, samt hur vi kan rikta läkemedel mot sjukliga tillstånd som orsakas av att en viss gen uttrycks i

för stor grad, eller tillverka effektivare diagnostiska metoder för att upptäcka sjukdomar på ett tidigt stadium.

Dessa studier började med att vi studerade hur sekvensen hos en enkla DNA- och RNA strängar påverkar basernas kemiska egenskaper genom att studera hur känsliga den utbytbara väteatomen på en av dessa baser (guanin) är mot höjt pH beroende av vilka baser den är omgiven av i sekvensen. Vi kunde se ett direkt samband mellan hur väl baserna stackade och hur skyddad väteatomen blev. Jag utvidgade sedan dessa experiment till att studera vilka strukturella skillnader som finns i stackningen av baserna mellan enkelsträngat DNA och RNA. Med hjälp av skillnaderna i spektra kunde jag fastslå att geometrin för stackningen mellan baser i enkelsträngat DNA och RNA har en väldigt snarlik trappstegsliknande struktur, men med den stora skillnaden att de leder i motsatta riktningar med hänsyn till deras sekvens. Denna upptäckt gör det möjligt att förklara skillnader vi sett i pH-känsligheten hos väteatomer i baser med olika grannbaser mellan enkelsträngat DNA och RNA.

Denna upptäckt kan även användas för att ge en möjlig förklaring till mekanismen bakom den så kallade "dangling end" effekten, vilket är den stabilisering man får genom att koppla på en kort enkelsträngad svans eller en enkel överhängande bas på en dubbelsträngad sekvens. Den stabilisering man får är helt beroende av vilken ände av dubbelsträngen man låter hänga över – i den ena änden får man en stark effekt medans den andra änden ger en väldigt svag effekt. Det intressanta med denna skillnad mellan ändarna är att effekten är helt omvänd om man jämför ändarna av DNA gentemot RNA. Genom att använda de observationer jag gjort för enkelsträngat DNA och RNA kunde jag härleda skillnaderna i den stabilitet man får av en överhängande bas till den geometri denna bas upptar över det sista basparet i den dubbelsträngade sekvensen. För att bevisa sambandet extraherade jag geometrin hos 105 publicerade strukturer med överhäng och jämförde hur väl den överhängande basen skyddar det yttersta basparet i den dubbelsträngade delen med den redan publicerade stabilisering man får av motsvande sekvens. På detta sätt kunde jag med hjälp av en databasstudie visa på ett direkt samband mellan hur väl det yttersta basparet skyddas mot det omgivande vattnet och den stabilitet man vinner, och därmed föreslå en mekanism bakom den ökade stabiliteten.

Målet med avhandlingen har varit att utöka vår förståelse för hur DNA och RNA fungerar, och hur vi kan föra detta fält frammåt och utveckla läkemedel mot- och diagnostik för genrelaterade sjukdomar.

7 References

(1)   Saenger, W. (1984) *Principles of Nucleic Acid Structure*, Springer-Verlag, New York.

(2)   Bloomfield, V. A., Crothers, D. M., and Tinoco, I. (1999) *Nucleic Acids: Structures, Properties and Functions*, University Science Books, Sausalito, California.

(3)   Felsenfeld, G., and Miles, H. T. (1967) The Physical and Chemical Properties of Nucleic Acids. *Annu. Rev. Biochem. 36*, 407-448.

(4)   Watson, J. D., and Crick, F. H. C. (1953) Molecular Structure of Nucleic Acids. A Structure for Deoxyribose Nucleic Acid. *Nature 171*, 737-738.

(5)   Zamenhof, S., Brawermann, G., and Chargaff, E. (1952) On the deoxypentose nucleic acids from several microorganisms. *Biochim. Biophys. Acta 9*, 402-405.

(6)   Furberg, S. (1950) The Crystal Structure of cytidine. *Acta Crystallogr. 3*, 325-331.

(7)   Cram, D. J. (1986) Preorganization - From Solvents to Spherands. *Angew. Chem. Int. Ed. 25*, 1039-1057.

(8)   Eichhorn, G. L., and Shin, Y. A. (1968) Interaction of metal ions with polynucleotides and related compounds. XII. The relative effect of various metal ions on DNA helicity. *J. Am. Chem. Soc. 90*, 7323-7328.

(9)   Tam, S.-C., and Williams, R. J. P. (1985) *Electrostatics in Biological Systems.*, Springer, Berlin, pp105-152.

(10)   Shoup, R. R., Miles, H. T., and Becker, E. D. (1966) NMR evidence of specific base-pairing between purines and pyrimidines. *Biochem. Biophys. Res. Comm. 23*, 194-201.

(11)   Hamlin, R. M. J., Lord, R. C., and Rich, A. (1965) Hydrogen-Bonded Dimers of Adenine and Uracil Derivatives. *Science 148*, 1734-1737.

(12)   Kyogoku, Y., Lord, R. C., and Rich, A. (1966) Hydrogen Bonding Specificity of Nucleic Acid Purines and Pyrimidines in Solution. *Science 154*, 518-520.

(13)   Maltseva, T. V., and Chattopadhyaya, J. (1995) Poor Hydration Enhances The Activation Energy of the Exchange Rate of the Base-paired Imino Protons with Water at the Core Part of the DNA Duplex. *Tetrahedron 51*, 5501-5508.

(14)   Leijon, M., and Gräslund, A. (1992) Effects of sequence and length on imino proton exchange and base pair opening kinetics in DNA oligonucleotide duplexes. *Nucl. Acids Res. 20*, 5339-5343.

(15)   Leroy, J. L., Kochoyan, M., Huynh-Dinh, T., and Guéron, M. (1988) Characterization of base-pair opening in deoxynucleotide duplexes using catalyzed exchange of the imino proton. *J. Mol. Biol. 200*, 223-238.

(16)   Pardi, A., Morden, K. M., Patel, D. J., and Tinoco, I. (1982) Kinetics for exchange of imino protons in the d(C-G-C-G-A-A-T-T-C-G-C-G) double helix and in two similar helices that contain a G.T base pair, d(C-G-T-G-A-A-T-T-C-G-C-G), and an extra adenine, d(C-G-C-A-G-A-A-T-T-C-G-C-G). *Biochemistry 21*, 6567-6574.

(17)   Pardi, A., Morden, K. M., Patel, D. J., and Tinoco, I. (1983) Kinetics for exchange of the imino protons of the d(C-G-C-G-A-A-T-T-C-G-C-G) double helix in complexes with the antibiotics netropsin and/or actinomycin. *Biochemistry 22*, 1107-1113.

(18)   Pardi, A., and Tinoco, I. (1982) Kinetics for exchange of imino protons in deoxyribonucleic acid, ribonucleic acid, and hybrid oligonucleotide helixes. *Biochemistry 21*, 4686-4693.

(19)   Guéron, M., Kochoyan, M., and Leroy, J. L. (1987) A single mode of DNA base-pair opening drives imino proton exchange. *Nature 328*, 89-92.

(20)   Maltseva, T., Sandström, A., Ivanova, I. M., Sergeyev, D. S., Zarytova, V. F., and Chattopadhyaya, J. (1993) Structural studies of the 5'-phenazinium-tethered matched and G-A-mismatched DNA duplexes by NMR spectroscopy. *J. Biochem. Biophys. Meth 26*, 173-236.

(21)   Becker, M., Lerum, V., Dickson, S., Nelson, N. C., and Matsuda, E. (1999) The Double Helix is Dehydrated: Evidence from the Hydrolysis of Acridinium Ester-Labeled Probes. *Biochemistry 38*, 5603-5611.

(22)   Pearlman, D. A., and Kim, S.-G. (1990) Atomic charges for DNA constituents derived from single-crystal X-ray diffraction data. *J. Mol. Biol. 211*, 171-187.

(23)   Sponer, J., Leszczynski, J., and Hobza, P. (2001) Electronic Properties, Hydrogen Bonding, Stacking, and Cation Binding of DNA and RNA Bases. *Biopolymers 61*, 3-31.

(24)   Sponer, J., Leszczynski, J., and Hobza, P. (2001) Hydrogen bonding, stacking and cation binding of DNA bases. *J. Mol. Struct. 573*, 43-53.

(25)   Sponer, J., Leszczynski, J., and Hobza, P. (1996) Structures and Energies of Hydrogen-Bonded DNA Base Pairs. A Nonemperical Study with Inclusion of Electron Correlation. *J. Phys. Chem. 100*, 1965-1974.

(26)   Pranata, J., Wierschke, S. G., and Jorgensen, W. L. (1991) OPLS Potential Functions for Nucleotide Bases. Relative Association Constants of Hydrogen-Bonded Base Pairs in Chloroform. *J. Am. Chem. Soc. 113*, 2810-2819.

(27)   Kyogoku, Y., Lord, R. C., and Rich, A. (1967) The Effect of Substituents on the Hydrogen Bonding of Adenine and Uracil Derivatives. *Proc. Natl. Acad. Sci. USA 57*, 250-257.

(28)   Sukhodub, L. F. (1987) Interactions and Hydration of Nucleic Acid Bases in a Vacuum. Experimental Study. *Chem. Rev. 87*, 589-606.

(29)   Jorgensen, W. L., and Pranata, J. (1990) Importance of Secondary Interactions in Triply Hydrogen Bonded Complexes: Guanine-Cytosine vs Uracil-2,6-Diaminopyridine. *J. Am. Chem. Soc. 112*, 2008-2010.

(30)   Popelier, P. L. A., and Joubert, L. (2002) The Elusive Atomic Rationale for DNA Base Pair Stability. *J. Am. Chem. Soc. 124*, 8725-8729.

(31)   Yang, J., and Gellman, S. H. (1998) Energetic Superiority of Two-Center Hydrogen Bonding Relative To Three-Center Hydrogen Bonding in a Model System. *J. Am. Chem. Soc. 120*, 9090-9091.

(32)   Hoogsteen, K. (1963) The Crystal and Molecular Structure of Hydrogen-bonded Complex Between 1-Methylthymine and 9-Methyladenine. *Acta Crystallogr. 16*, 907-916.

(33)   Kim, S.-G. (1976) Three-dimensional structure of transfer RNA. *Prog. Nucl. Acid Res. Mol. Biol. 17*, 181-216.

(34)   Sussman, J. L., Holbrook, S. R., Wade Warrant, R., Church, G. M., and Kim, S.-G. (1978) Crystal Structure of yeast phenylalanine tRNA. I. Crystallographic refinement. *J. Mol. Biol. 123*, 607-630.

(35)   Wimberly, B., Varani, G., and Tinoco, I. J. (1993) The Conformation of Loop E of Eukaryotic 5S Ribosomal RNA. *Biochemistry 32*, 1078-1087.

(36)   Noller, H. F. (1984) Structure of Ribosomal RNA. *Annu. Rev. Biochem. 53*, 119-162.

(37)   Christophe, D., Cabrer, B., Bacolla, A., Targovnik, H., Pohl, V., and Vassart, G. (1985) An unusually long poly(purine)-poly(pyrimidine) sequence is located upsteam from the human thyroglobulin gene. *Nucl. Acids Res. 13*, 5127-5144.

(38)   Mirkin, S. M., Lyamichev, V. I., Drushlyak, K. N., Dobrynin, V. N., Filippov, S. A., and Frank-Kamenetskii, M. D. (1987) DNA H form requires a homopurine-homopyrimidine mirror repeat. *Nature 330*, 495-497.

(39)   Stevens, C. L., and Felsenfeld, G. (1964) The Conversion of Two-stranded Poly (A+U) to Three-strand Poly (A+2U) and Poly A by Heat. *Biopolymers 2*, 293-314.

(40)   Lipsett, M. N. (1963) The Interactions of Poly C and Guanine Trinucleotide. *Biochem. Biophys. Res. Comm. 11*, 224-228.

(41)   Lipsett, M. N. (1964) Complex Formation between Polycytidylic Acid and Guanine Oligonucleotides. *J. Biol. Chem. 239*, 1256-1260.

(42)   Felsenfeld, G., Davies, D. R., and Rich, A. (1957) Formation of a Three-Stranded Polynucleotide Molecule. *J. Am. Chem. Soc. 79*, 2023-2024.

(43)   Phillips, K., Dauter, Z., Murchie, A. I. H., Lilley, D. M. J., and Luisi, B. (1997) The Crystal Structure of a Parallel-stranded Guanine Tetraplex at 0.95 Å Resolution. *273*, 171-182.

(44)   Diekmann, T., Suzuki, E., Nakamura, G. K., and Feigon, J. (1996) Solution structure of an ATP-binding RNA aptamer reveals a novel fold. *RNA 2*, 628-640.

(45)   Sen, D., and Gilbert, W. (1988) Formation of Parallel Four-Stranded Complexes by Guanine-rich Motifs in DNA and its Implications for Meiosis. *Nature 334*, 364-366.

(46)   Williamson, J. R., Raghuraman, M. K., and Cech, T. R. (1989) Monovalent Cation-Induced Structure of Telomeric DNA: The G-Quartet Model. *Cell 59*, 871-880.

(47)   Sen, D., and Gilbert, W. (1990) A Sodium-Potassium Switch in the Formation of Four-Stranded G4-DNA. *Nature 344*, 410-414.

(48)   Kim, J., Cheong, C., and Moore, P. B. (1991) Tetramerization of an RNA Oligonucleotide Containing a GGGG Sequence. *Nature 351*, 331-332.

(49)   Macaya, R. F., Schultze, P., Smith, F. W., Roe, J. A., and Feigon, J. (1993) Thrombin-binding DNA aptamer forms a unimolecular quadruplex structure in solution. *Proc. Natl. Acad. Sci. USA 90*, 3745-3749.

(50)   Rich, A., Davies, D. R., Crick, F. H. C., and Watson, J. D. (1961) The Molecular Structure of Polyadenylic Acid. *J. Mol. Biol. 3*, 71-86.

(51)   Hunter, W. N., Brown, T., Anand, N. K., and Kennard, O. (1986) Structure of an Adenine.Cytosine Base Pair in DNA and Its Implications for Mismatch Repair. *Nature 320*, 552-555.

(52)   Hunter, W. N., Brown, T., and Kennard, O. (1987) Structural Features and Hydration of a Dodecamer Duplex Containing Two C.A Mispairs. *Nucl. Acids Res. 15*, 6589-6606.

(53)   Kalnik, M. W., Kouchakdjian, M., Li, B. F. L., Swann, P. F., and Patel, D. J. (1988) Base Pair Mismatches and Carcinogen-Modified Bases in DNA: An NMR Study of A.C and A.O^{4}meT Pairing in Dodecanucleotide Duplexes. *Biochemistry 27*.

(54)   Borah, B., and Wood, J. L. (1976) The Cytidinium-cytidine Complex: Infrared and Raman Spectroscopic Studies. *J. Mol. Struct. 30*, 13-30.

(55)   Pilch, D. S., and Shafer, R. H. (1993) Structural and thermodynamic studies of d(C$_3$T$_4$C$_3$) in acid solution - evidence for formation of the hemiprotonated CH$^+$.C base pair. *J. Am. Chem. Soc. 115*, 2565-2571.

(56)   Sundquist, W. I., and Klug, A. (1989) Telomeric DNA Dimerizes by Formation of Guanine Tetrads Between Hairpin Loops. *Nature 342*, 825-829.

(57)   Shan, S.-o., Loh, S., and Herschlag, D. (1996) The Energetics of Hydrogen Bonds in Model Systems: Implications for Enzymatic Catalysis. *Science 272*, 97-101.

(58)   Shan, S.-o., and Herschlag, D. (1996) The change in hydrogen bond strength accompanying charge rearrangement: Implications for enzymatic catalysis. *Biochemistry 93*, 14474-14479.

(59)   Hunter, C. A., Lawson, K. R., Perkins, J., and Urch, C. J. (2001) Aromatic interactions. *J. Chem. Soc. Perkin Trans. 2*, 651-669.

(60)   Hunter, C. A., and Sanders, J. K. M. (1990) The Nature of $\pi-\pi$ Interactions. *J. Am. Chem. Soc. 112*, 5525-5534.

(61)   West, A. P. J., Mecozzi, S., and Dougherty, D. A. (1997) THEORETICAL STUDIES OF THE SUPRAMOLECULAR SYNTHON BENZENE · · · HEXAFLUOROBENZENE. *J. Phys. Org. Chem. 10*, 347-350.

(62)   Kim, E.-i., Paliwal, S., and Wilcox, C. S. (1998) Measurements of Molecular Electrostatic Field Effects in Edge-to-Face Aromatic Interactions with Implications for Protein Folding and Molecular Recognition. *J. Am. Chem. Soc. 120*, 11192-11193.

(63)   Paliwal, S., Geib, S., and Wilcox, C. S. (1994) Molecular Torsion Balance for Weak Molecular Recognition Forces. Effects of "Tilted-T" Edge-to-Face Aromatic Interactions on Conformational Selection and Solid-State Structure. *J. Am. Chem. Soc. 116*, 4497-4498.

(64)   Suezawa, H., Hashimoto, T., Tsuchinaga, K., Yoshida, T., Yuzuri, T., Sakakibara, K., Hirota, M., and Nishio, M. (2000) Electronic substituent effect on intramolecular CH/π interaction as evidenced by NOE experiments. *J. Chem. Soc. Perkin Trans. 2 6*, 1243-1249.

(65)   Umezawa, Y., and Nishio, M. (2002) Thymine-methyl/π interaction implicated in the sequence-dependent deformability of DNA. *Nucl. Acids Res. 30*, 2183-2192.

(66)   Umezawa, Y., Tsuboyama, S., Takahashi, H., Uzawa, J., and Nishio, M. (1999) CH/π Interaction in the Conformation of Organic Compounds. A Database Study. *Tetrahedron 55*, 10047-10056.

(67)   Mascal, M., Armstrong, A., and Bartberger, M. D. (2002) Anion-Aromatic Bonding: A Case for Anion Recognition by π-Acidic Rings. *J. Am. Chem. Soc. 124*, 6274-6276.

(68)   Gale, P. A., Navakhun, K., Camiolo, S., Light, M. E., and Hursthouse, M. B. (2002) Anion-Anion Assembly: A New Class of Anionic Supramolecular Polymer Containing 3,4-Dichloro-2,5-diamido-substituted Pyrrole Anion Dimers. *J. Am. Chem. Soc. 124*, 11228.

(69)   Ma, J. C., and Dougherty, D. A. (1997) The Cation-π Interaction. *Chem. Rev. 97*, 1303-1324.

(70)   Quiñonero, D., Garau, C., Rotger, C., Frontera, A., Ballester, P., Costa, A., and Deyà, P. M. (2002) Anion-π Interactions: Do They Exist? *Angew. Chem. Int. Ed. 41*, 3389-3392.

(71)   Garau, C., Quiñonero, D., Frontera, A., Ballester, P., Costa, A., and Deyà, P. M. (2003) Anion-π interactions: must the aromatic ring be electron deficient? *New. J. Chem. 27*, 211-214.

(72)   Cozzi, F., Cinquini, M., Annuziata, R., Dwyer, T., and Siegel, J. S. (1992) Polar/π Interactions between Stacked Aryls in 1,8-Diarylnaphthalenes. *J. Am. Chem. Soc. 114*, 5729-5733.

(73)   Cozzi, F., Cinquini, M., Annuziata, R., and Siegel, J. S. (1993) Dominance of Polar/π over Charge-Transfer Effects in Stacked Phenyl Interactions. *J. Am. Chem. Soc. 115*, 5330-5331.

(74)   Hunter, C. A. (1993) Sequence-dependent DNA Structure - The role of Base Stacking Interactions. *J. Mol. Biol. 230*, 1025-1054.

(75)   Carreira, L. A., Jiang, G. J., and Person, W. B. (1972) Spectroscopic Determination of the Barrier to Planarity in Cyclopentane. *J. Chem. Phys. 56*, 1440-1443.

(76)   Kilpatrick, J. E., Pitzer, K. S., and Spitzer, R. (1947) The Thermodynamics and Molecular Structure of Cyclopentane. *J. Am. Chem. Soc. 69*, 2483-2488.

(77)   Altona, C., and Sundaralingam, M. (1972) Conformational Analysis of the Sugar Ring in Nucleosides and Nucleotides. A New Description Using the Concept of Pseudorotation. *J. Am. Chem. Soc. 94*, 8205-8212.

(78)   Altona, C., and Sundaralingam, M. (1973) Conformational Analysis of the Sugar Ring in Nucleosides and Nucleotides. Improved Method for the Interpretation of Proton Magnetic Resonance Coupling Constants. *J. Am. Chem. Soc. 95*, 2333-2344.

(79)   Strauss, H. L. (1983) PSEUDOROTATION: A Large Amplitude Molecular Motion. *Ann. Rev. Phys. Chem. 34*, 301-328.

(80)   IUPAC-IUB. (1983) Abbreviations and Symbols for the Description of Conformations of Polynucleotide Chains. Recommendations 1982. *Eur. J. Biochem. 131*, 9-15.

(81)   IUPAC-IUB. (1976) Rules for the nomenclature of organic chemistry, Section E: Stereochemistry, Recommendations 1974. *Pure Appl. Chem. 45*, 11-30.

(82)   Kitamura, K., Wakahara, A., Mizuno, H., Baba, Y., and Tomita, K.-I. (1981) Conformationally "concerted" changes in nucleotide structures. A new description using circular correlation and regression analyses. *J. Am. Chem. Soc. 103*, 3899-3904.

(83)   Yathindra, N., and Jayaraman, S. (1983) From nucleotides to nucleosomes - stereochemical approaches to probe the adaptability of the backbone conformations in nucleic acids. *Conform. Biol.*, 299-312.

(84)   Olson, W. K., Bansal, M., Burley, S. K., Dickerson, R. E., Gerstein, M., Harvey, S. C., Heinemann, U., Lu, X. J., Neidle, S., Shakked, Z., Sklenar, H., Suzuki, M., Tung, C. S., Westhof, E., Wolberger, C., and Berman, H. M. (2001) A standard reference frame for the description of nucleic acid base-pair geometry. *J. Mol. Biol. 313*, 229-237.

(85)   Gorin, A. A., Zhurkin, V. B., and Olson, W. K. (1995) B-DNA twisting correlates with base-pair morphology. *J. Mol. Biol. 247*, 34-48.

(86)   Kosikov, K. M., Gorin, A. A., Zhurkin, V. B., and Olson, W. K. (1999) DNA stretching and compression: large-scale simulations of double helical structures. *J. Mol. Biol. 289*, 1301-1326.

(87)   Lavery, R., and Sklenar, H. (1988) The definition of generalized helicoidal parameters and of axis curvature for irregular nucleic acids. *J. Biomol. Struct. Dyn. 6*, 63-91.

(88)   Babcock, M. S., Pednault, E. P., and Olson, W. K. (1993) Nucleic acid structure analysis: a users guide to a collection of new analysis programs. *J. Biomol. Struct. Dyn. 11*, 597-628.

(89)   Lu, X.-J., and Olson, W. K. (2003) 3DNA: a software package for the analysis, rebuilding and visualization of three-dimensional nucleic acid structure. *Nucl. Acids Res. 31*, 5108-5121.

(90)   Kennard, O., and Hunter, W. N. (1989) Oligonucleotide Structure - A Decade of Results From Single Crystal X-Ray Diffraction Studies. *Q. Rev. Biophys. 22*, 327-379.

(91)   Leslie, A. G. W., Arnott, S., Chandrasekaran, R., and Ratliff, R. L. (1980) Polymorphism of DNA double helices. *J. Mol. Biol. 143*, 49-72.

(92)   Arnott, S., Chandrasekaran, R., Puigjaner, L. C., Walker, J. K., Hall, I. H., Birdsall, D. L., and Ratliff, R. L. (1983) Wrinkled DNA. *Nucl. Acids Res. 11*, 1457-1474.

(93)   Arnott, S., and Hukins, D. W. (1973) Refinement of the Structure of B-DNA and Implications for the Analysis of X-Ray Diffraction Data from Fibers of Biopolymers. *J. Mol. Biol. 81*, 93-105.

(94)   Wang, A. H.-J., Quigley, G. J., Kolpak, F. J., Crawford, J. L., van Boom, J. H., van der Marel, G., and Rich, A. (1979) Molecular Structure of a Left-Handed Double Helical DNA Fragment at Atomic Resolution. *Nature 282*, 680-686.

(95)   Dickerson, R. E. (1992) DNA structure from A to Z. *Methods Enzymol. 211*, 67-111.

(96)   Ivanov, V. I., Minchenkova, L. E., Minyat, E. E., Frank-Kamenetskii, M. D., and Schyolkina, A. K. (1974) The B to A transition of DNA in solution. *J. Mol. Biol. 87*, 817-833.

(97)   Ivanov, V. I., Minchenkova, L. E., Schyolkina, A. K., and Poletayev, A. I. (1973) Different conformations of double-stranded nucleic acid in solution as revealed by circular dichroism. *Biopolymers 12*, 89-110.

(98)   Doucet, J., Benoit, J. P., Cruse, W. B., Prange, T., and Kennard, O. (1989) Coexistance of A- and B-form DNA in a single crystal lattice. *Nature 337*, 190-192.

(99)   Trulson, M. O., Cruz, P., Puglisi, J. D., Tinoco, I., and Mathies, R. A. (1987) Raman Spectroscopic Study of Left-handed Z-RNA. *Biochemistry 26*, 8624-8630.

(100)   Pohl, F. M., and Jovin, T. M. (1972) Salt-induced Co-operative Conformational Change of a Synthetic DNA: Equilibrium and Kinetic Studies with Poly(dG-dC). *J. Mol. Biol. 67*, 375-396.

(101)   Behe, M., and Felsenfeld, G. (1981) Effects of methylation on a synthetic polynucleotide: The B-Z transition in poly(dG-m5dC):poly(dG-m5dC). *Proc. Natl. Acad. Sci. USA 78*, 1619-1623.

(102)   Ansevin, A. T., and Wang, A. H. (1990) Evidence for a new Z-type left handed DNA helix: Properties of Z(WC)-DNA. *Nucl. Acids Res. 18*, 6119-6126.

(103)   Davidson, E. R., and Feller, D. (1984) Molecular properties of water. *Chem. Phys. Lett. 104*, 54-58.

(104)   Falk, M., Hartman, K. A. J., and Lord, R. C. (1963) Hydration of deoxyribonucleic acid. II. An infrared study. *J. Am. Chem. Soc. 85*, 387-391.

(105)   Falk, M., Poole, A. G., and Goymour, C. G. (1970) Infrared study on the state of water in the hydration shell of DNA. *Can. J. Chem. 48*, 1536-1542.

(106)   Falk, M., Hartman, K. A. J., and Lord, R. C. (1962) Hydration of deoxyribonucleic acid. I. A gravimetric study. *J. Am. Chem. Soc. 84*, 3843-3846.

(107)   Gray, D. M., Bloomfield, V. A., and Hearst, J. E. (1967) Sedimentation coefficients of linear and cyclic wormlike chains with excluded volume effects. *J. Chem. Phys. 46*, 1493-1498.

(108)   Wang, J. H. (1955) The hydration of deoxyribonucleic acid. *J. Am. Chem. Soc. 77*, 258-260.

(109)   Privalov, P. L., and Mrevlishvili, G. M. (1967) Macromolecule hydration in native and denatured state. *Biofizika 12*, 22-29.

(110)   Kuntz, I. D. J., Brassfield, T. S., Law, G. D., and Purcell, G. V. (1969) Hydration of macromolecules. *Science 163*, 1329-1331.

(111)   Drew, H. R., and Dickerson, R. E. (1981) Structure of a B-DNA dodecamer III. Geometry of hydration. *J. Mol. Biol. 151*, 535-556.

(112)   Kopka, M. L., Fratini, A. V., Drew, H. R., and Dickerson, R. E. (1983) Ordered water structure around a B-DNA dodecamer. A quantitative study. *J. Mol. Biol. 163*, 129-146.

(113)   Liepinsh, E., Otting, G., and Wüthrich, K. (1992) NMR observation of individual molecules of hydration water bound to DNA duplexes: direct evidence for a spine of hydration water present in aqueous solution. *Nucl. Acids Res. 20*, 6549-6553.

(114)   Denisov, V. P., Carlström, G., Venu, K., and Halle, B. (1997) Kinetics of DNA Hydration. *J. Mol. Biol. 268*, 118-136.

(115) Berman, H. M. (1994) Hydration of DNA: take 2. *Curr. Op. Struct. Biol. 4*, 345-350.

(116) Heinemann, U., and Alings, C. (1989) Crystallographic study of one turn of GC-rich B-DNA. *J. Mol. Biol. 210*, 369-381.

(117) Lipanov, A., Kopka, M. L., Kaczor-Grzeskowiak, M., Quintana, J., and Dickerson, R. E. (1993) Structure of the B-DNA decamer C-C-A-A-C-I-T-T-G-G in two different space groups: Conformational flexibility of B-DNA. *Biochemistry 32*, 1373-1389.

(118) Privé, G. G., Yanagi, K., and Dickerson, R. E. (1991) Structure of the B-DNA decamer C-C-A-A-C-G-T-T-G-G and comparison with isomorphous decamers C-C-A-A-G-A-T-T-G-G and C-C-A-G-G-C-C-T-G-G. *J. Mol. Biol. 217*, 177-199.

(119) Privé, G. G., Heinemann, U., Chandrasegaran, S., Kan, L.-S. M., Kopka, L., and Dickerson, R. E. (1987) Helix Geometry, Hydration, and G.A Mismatch in a B-DNA Decamer. *Science 238*, 498-504.

(120) Quintana, J. R., Grzeskowiak, K., Yanagi, K., and Dickerson, R. E. (1992) Structure of a B-DNA decamer with a central T-A step: C-G-A-T-T-A-A-T-C-G. *J. Mol. Biol. 225*, 379-395.

(121) Govil, G., and Saran, A. (1971) Quantum chemical studies on the conformational structure of nucleic acids. II. EHT and CNDO calculations on the puckering of D-ribose. *J. Theor. Biol. 33*, 399-406.

(122) Lugovskoi, A. A., and Dashevskii, V. G. (1972) Conformations of β-D-ribose. *Mol. Biol. 6*, 354-360.

(123) Lugovskoi, A. A., Dashevskii, V. G., and Kitaigorodskii, A. I. (1972) Conformations of of sugar residues in pyrimidine nucleosides. *Mol. Biol. 6*, 361-367.

(124) Lugovskoi, A. A., Dashevskii, V. G., and Kitaigorodskii, A. I. (1972) Conformations of sugar residues in purine nucleosides. *Mol. Biol. 6*, 494-499.

(125) Levitt, M., and Warshel, A. (1978) Extreme conformational flexibility of the furanose ring in DNA and RNA. *J. Am. Chem. Soc. 100*, 2607-2613.

(126) Brameld, K. A., and Goddard III, W. A. (1999) Ab Initio Quantum Mechanical Study of the Structures and Energies for the Pseudorotation of 5'-Dehydroxy Analogues of 2'-Deoxyribose and Ribose Sugars. *J. Am. Chem. Soc. 121*, 985-993.

(127) Foloppe, N., and MacKerell, D. J. (1999) Intrinsic Conformational Properties of Deoxyribonucleosides: Implicated Role for Cytosine in the Equilibrium Among the A, B, and Z Forms of DNA. *Biophys. J. 76*, 3206-3218.

(128) Olson, W. K. (1982) How Flexible Is the Furanose Ring? 2. An Updated Potential Energy Estimate. *J. Am. Chem. Soc. 104*, 278-286.

(129) Pearlman, D. A., and Kim, S.-H. (1985) Conformational Studies on Nucleic Acids II. The Conformational Energetics of Commonly Occuring Nucleosides. *J. Biomol. Struct. Dyn. 3*, 99-125.

(130) Arora, K., and Schlick, T. (2003) Deoxyadenosine sugar puckering pathway simulated by the stochastic difference equation algorithm. *Chem. Phys. Lett. 378*, 1-8.

(131) Meints, G. A., Karlsson, T., and Drobny, G. P. (2001) Modeling Furanose Ring Dynamics in DNA. *J. Am. Chem. Soc. 123*, 10030-10038.

(132)   Röder, O., Lüdemann, H.-D., and von Goldammer, E. (1975) Determination of the Activation Energy for Pseudorotation of the Furanose Ring in Nucleosides by 13C Nuclear-Magnetic-Resonance Relaxation. *Eur. J. Biochem. 53*, 517-524.

(133)   Elber, R., Cardenas, A., Ghosh, A., and Stern, H. A. (2003) Bridging the gap between long time trajectories and reaction pathways. *Adv. Chem. Phys. 126*, 93-129.

(134)   Harvey, S. C., and Prabhakaran, M. (1986) Ribose puckering: structure, dynamics, energetics, and the pseudorotation cycle. *J. Am. Chem. Soc. 108*, 6128-6136.

(135)   Gabb, H. A., and Harvey, S. C. (1993) Conformational transitions in potential and free energy space for furanoses and 2'-deoxynucleosides. *J. Am. Chem. Soc. 115*, 4218-4227.

(136)   Perrin, C. L., Armstrong, K. B., and Fabian, M. A. (1994) The origin of the anomeric effect: conformational analysis of 2-methoxy-1,3-dimethylhexahydropyrimidine. *J. Am. Chem. Soc. 116*, 715-722.

(137)   Koole, L. H., Buck, H. M., Nyilas, A., and Chattopadhyaya, J. (1987) Structural properties of modified deoxyadenosine structures in solution. Impact of the gauche and anomeric effects on the furanose conformation. *Can. J. Chem. 65*, 2089-2094.

(138)   Plavec, J., Tong, W., and Chattopadhyaya, J. (1993) How do the gauche and anomeric effects drive the pseudorotational equilibrium of the pentofuranose moiety of nucleosides? *J. Am. Chem. Soc. 115*, 9734-9746.

(139)   Luyten, I., Thibaudeau, C., and Chattopadhyaya, J. (1997) The Strength of the Anomeric Effect in Adenosine, Guanosine, and in Their 2'-Deoxy Counterparts is Medium-Dependent. *J. Org. Chem. 62*, 8800-8808.

(140)   Thibaudeau, C., and Chattopadhyaya, J. (1999) *Stereoelectronic Effects in Nucleosides and Nucleotides and their Structural Implications*, Uppsala University Press, Uppsala, Sweden.

(141)   Thibaudeau, C., Plavec, J., and Chattopadhyaya, J. (1996) Quantitation of the pD Dependent Thermodynamics of the N-S Pseudorotational Equilibrium of the Pentofuranose Moiety in Nucleosides Gives a Direct Measurement of the Strength of the Tunable Anomeric Effect and the pKa of the Nucleobase. *J. Org. Chem. 61*, 266-286.

(142)   Plavec, J., Thibaudeau, C., and Chattopadhyaya, J. (1996) How do the energetics of the stereoelectronic gauche and anomeric effects modulate the conformation of nucleosides and nucleotides. *Pure Appl. Chem. 68*, 2137-2144.

(143)   Plavec, J., Thibaudeau, C., and Chattopadhyaya, J. (1994) How Does the 2'-Hydroxy Group Drive the Pseudorotational Equilibrium in Nucleoside and Nucleotide by the Tuning of the 3'-Gauche Effect? *J. Am. Chem. Soc. 116*, 6558-6560.

(144)   Dionne, P., and St-Jacques, M. (1987) Mechanism of the gauche conformational effect in 3-halogenated 1,5-benzodioxepins. *J. Am. Chem. Soc. 109*, 2616-2623.

(145)   Wiberg, K. B. (1996) Bent Bonds in Organic Compounds. *Acc. Chem. Res. 29*, 229-234.

(146) Thibaudeau, C., Plavec, J., Garg, N., Papchikhin, A., and Chattopadhyaya, J. (1994) How does the 3'-phosphate drive the sugar conformation in DNA? *J. Am. Chem. Soc. 116*, 4038-4043.

(147) Miha, P., Cmugelj, M., Stimac, A., Kobe, J., and Plavec, J. (2001) 8-Aza-3-deazaguanine modification strengthens the anomeric effect and affects other conformational preferences of modified guanine nucleosides. *J. Chem. Soc. Perkin Trans. 2 8*, 1433-1438.

(148) Rosemeyer, H., and Seela, F. (1997) Stereoelectronic effects of modified purine bases on the sugar conformation of nucleosides: pyrrolo[2,3-d]pyrimidines. *J. Chem. Soc. Perkin Trans. 2 11*, 2341-2346.

(149) Guschlbauer, W., and Jankowski, K. (1980) Nucleoside conformation is determined by the electronegativity of the sugar substituent. *Nucl. Acids Res. 8*, 1421-1433.

(150) Uesugi, S., Kaneyasu, T., Imura, J., Ikehara, M., Cheng, D. M., Kan, L., and Ts'o, P. O. P. (1983) Proton-NMR studies on the dinucleoside mono-phosphates containing 2'-halogeno-2'-deoxypurinenucleosides: effects of 2'-substituents on conformation. *Biopolymers 22*, 1189-1202.

(151) van den Boogaart, J. E., Kalinichenko, E. N., Podkopaeva, T. L., Mik-hailopulo, I. A., and Altona, C. (1994) Conformational analysis of 3'-fluorinated A(2'-5')A(2'-5')A fragments. Relation between conformation and biological activity. *Eur. J. Biochem. 221*, 759-768.

(152) Patel, D. J., Ikuta, S., Kozlowski, S., and Itakura, K. (1983) Sequence De-pendence of Hydrogen Exchange Kinetics in DNA Duplexes at the Indi-vidual Base Pair Level in Solution. *Proc. Natl. Acad. Sci. USA 80*, 2184-2188.

(153) Maltseva, T. V., Altmann, K.-H., Egli, M., and Chattopadhyaya, J. (1998) The Residence Time of the Bound Water in the Hydrophobic Minor Groove of the Carbocyclic-Nucleoside Analogs of Dickerson-Drew Dode-camers. *J. Biomol. Struct. Dyn. 16*, 569-578.

(154) Dhavan, G. M., Lapham, J., Yang, S., and Crothers, D. M. (1999) De-creased Imino Proton Exchange and Base-pair Opening in the IHF-DNA Complex Measured by NMR. *J. Mol. Biol. 288*, 659-671.

(155) Maltseva, T. V., Yamakage, S. I., Agback, P., and Chattopadhyaya, J. (1993) Direct estimation of base-pair exchange kinetics in oligo-DNA by a combination of NOESY and ROESY experiments. *Nucl. Acids Res. 21*, 4288-4295.

(156) Pardi, A., Morden, K. M., Patel, D. J., and Tinoco, I. (1983) Kinetics for exchange of imino protons in the d(C-G-C-G-A-A-T-T-C-G-C-G) double helix and in two similar helices that contain a G.T base pair, d(C-G-T-G-A-A-T-T-C-G-C-G), and an extra adenine, d(C-G-C-A-G-A-A-T-T-C-G-C-G). *Biochemistry 21*, 6567-6574.

(157) Maltseva, T., Zarytova, V. F., and Chattopadhyaya, J. (1995) Base-pair exchange kinetics of the imino and amino protons of the 3'-phenazinium tethered DNA-RNA duplex, r(5'GAUUGAA3'):d(5'TCAATC3'-Pzn), and their comparison with those of B-DNA duplex. *J. Biochem. Biophys. Meth 30*, 163-177.

64

(158) Crothers, D. M., Cole, P. E., Hilbers, C. W., and Shulman, G. (1974) Kinetics for exchange of imino protons in deoxyribonucleic acid, ribonucleic acid, and hybrid oligonucleotide helixes. *J. Mol. Biol. 87*, 63-88.

(159) Johnston, P. D., and Redfield, A. G. (1977) An NMR study of the exchange rates for protons involved in the secondary and tertiary structure of yeast tRNA Phe. *Nucl. Acids Res. 4*, 3599-3615.

(160) Johnston, P. D., and Redfield, A. G. (1978) Pulsed FT-NMR double resonance studies of yeast tRNAPhe: specific nuclear Overhauser effects and reinterpretation of low temperature relaxation data. *Nucl. Acids Res. 5*, 3913-3927.

(161) Hurd, R. E., and Reid, B. R. (1980) Helix-coil dynamics in RNA: The amino acid acceptor helix of Escherichia coli phenylalanine transfer RNA. *J. Mol. Biol. 142*, 181-193.

(162) Gralla, J., and Crothers, D. M. (1973) Free energy of imperfect nucleic acid helices III. Small internal loops resulting from mismatches. *J. Mol. Biol. 78*, 301-306.

(163) Kao, S.-C., Polnaszek, C. F., Toppin, C. R., and Bobst, A. M. (1983) Internal Motions in Ribonucleic Acid Duplexes As Determined by Electron Spin Resonance with Site-Specifically Spin-Labeled Uridines. *Biochemistry 22*, 5563-5568.

(164) Bobst, A. M., Kao, S.-C., Toppin, R. C., Ireland, J. C., and Thomas, I. E. (1984) Dipsticking the major groove of DNA with enzymatically incorporated spin-labeled deoxyuridines by electron spin resonance spectroscopy. *J. Mol. Biol. 173*, 63-74.

(165) Kao, S.-C., and Bobst, A. M. (1985) Local Base Dynamics and Local Structural Features in RNA and DNA Duplexes. *Biochemistry 24*, 5465-5469.

(166) Assa-Munt, N., Granot, J., Behling, R. W., and Kearns, D. R. (1984) Proton NMR relaxation studies of the hydrogen-bonded imino protons of poly(dA-dT). *Biochemistry 23*, 944-955.

(167) Wang, A. C., Kennedy, M. A., Reid, B. R., and Drobny, G. (1994) A Solid-State 2H NMR Investigation of Purine Motion in a 12-Base-Pair RNA Duplex. *J. Magn. Reson. B 105*, 1-10.

(168) Wang, A. C., Kennedy, M. A., Reid, B. R., and Drobny, G. (1992) A Solid-State 2H NMR Relaxation Study of a 12 Base Pair RNA Duplex. *J. Am. Chem. Soc. 114*, 6583-6585.

(169) Kintanar, A., Huang, W. C., Schindele, D. C., Wemmer, D. E., and Drobny, G. (1989) Dynamics of bases in hydrated [d(CGCGAATTCGCG)]2. *Biochemistry 28*, 282-293.

(170) Patkowski, A., Eimer, W., and Dorfmüller, T. (1990) Internal dynamics of tRNA[Phe] studied by depolarized dynamic light scattering. *Biopolymers 30*, 975-983.

(171) Calogero, A., Hospers, G. A. P., and Mulder, N. H. (1997) Synthetic oligonucleotides: Useful molecules? A review. *Pharm. World Sci. 19*, 264-268.

(172) Lebedeva, I., and Stein, C. A. (2001) ANTISENSE OLIGONUCLEOTIDES: Promise and Reality. *Ann. Rev. Pharmacol. Toxicol. 41*, 403-419.

(173)   Micklefield, J. (2001) Backbone Modification of Nucleic Acids: Synthesis, Structure and Therapeutic Applications. *Curr. Med. Chem. 8*, 1157-1179.

(174)   Zamaratski, E., Pradeepkumar, P. I., and Chattopadhyaya, J. (2001) A critical survey of the structure-function of the antisense oligo/RNA heteroduplex as substrate for RNase H. *J. Biochem. Biophys. Meth. 48*, 189-208.

(175)   Minshull, J., and Hunt, T. (1986) The use of single-stranded DNA and RNase H to promote quantitative 'hybrid arrest of translation' of mRNA/DNA hybrids in reticulocyte lysate cell-free translations. *Nucl. Acids Res. 14*, 6433-6451.

(176)   Walder, R. Y., and Walder, J. A. (1988) Role of RNase H in Hybrid-Arrested Translation by Antisense Oligonucleotides. *Proc. Natl. Acad. Sci. USA 85*, 5011-5015.

(177)   Santoro, S. W., and Joyce, G. F. (1997) A general purpose RNA-cleaving DNA enzyme. *Proc. Natl. Acad. Sci. USA 94*, 4262-4266.

(178)   Breaker, R. R., and Joyce, G. F. (1994) A DNA enzyme that cleaves RNA. *Chem. Biol. 1*, 223-229.

(179)   Breaker, R. R., and Joyce, G. F. (1995) A DNA enzyme with Mg2+-dependent RNA phosphoesterase activity. *Chem. Biol. 2*, 655-660.

(180)   Cuenoud, B., and Szostak, J. W. (1995) A DNA metalloenzyme with DNA ligase activity. *Nature 375*, 611-614.

(181)   Kruger, K., Grabowski, P. J., Zaug, A. J., Sands, J., Gottschling, D. E., and Cech, T. R. (1982) Self-splicing RNA: Autoexcision and autocyclization of the ribosomal RNA intervening sequence of tetrahymena. *Cell 31*, 147-157.

(182)   Guerrier-Takada, C., Gardiner, K., Marsh, T., Pace, N., and Altman, S. (1983) The RNA moiety of ribonuclease P is the catalytic subunit of the enzyme. *Cell 35*, 849-857.

(183)   Christoffersen, R. E., and Marr, J. J. (1995) Ribozymes as Human Therapeutic Agents. *J. Med. Chem. 38*, 2023-2037.

(184)   Eder, P. S., DeVine, R. J., Dagle, J. M., and Walder, J. A. (1991) Substrate specificity and kinetics of degradation of antisense oligonucleotides by a 3' exonuclease in plasma. *Antisense Res. Dev. 1*, 141-151.

(185)   Vaerman, J. L., Moureau, P., Deldime, F., Lewalle, P., Lammineur, C., Morschhauser, F., and Martiat, P. (1997) Antisense Oligodeoxyribonucleotides Suppress Hematologic Cell Growth Through Stepwise Release of Deoxyribonucleotides. *Blood 90*, 331-339.

(186)   Akhtar, S., Basu, S., Wickstrom, E., and Juliano, R. L. (1991) Interactions of antisense DNA oligonucleotide analogs with phospholipid membranes (liposomes). *Nucl. Acids Res. 19*, 5551-5559.

(187)   Miller, P. S., and Ts'o, P. O. (1987) A new approach to chemotherapy based on molecular biology and nucleic acid chemistry: Matagen (masking tape for gene expression). *Anticancer Drug Des. 2*, 117-128.

(188)   Nielsen, P. E. (2000) Antisense peptide nucleic acids. *Curr. Op. Mol. Therapeut. 2*, 282-287.

(189)   Egholm, M., Buchardt, O., Christensen, L., Behrens, C., Freier, S. M., Driver, D. A., Berg, R. H., Kim, S. K., Norden, B., and Nielsen, P. E. (1993) PNA hybridizes to complementary oligonucleotides obeying the Watson-Crick hydrogen-bonding rules. *Nature 365*, 566-568.

(190) Nielsen, P. E., Egholm, M., Berg, R. H., and Buchardt, O. (1991) Sequence-selective recognition of DNA by strand displacement with a thymine-substituted polyamide. *Science 254*, 1497-1500.

(191) Angerer, L. M., and Angerer, R. C. (2004) Disruption of gene function using antisense morpholinos. *Methods Cell Biol. 74*, 699-711.

(192) Heasman, J. (2002) Morpholino Oligos: Making Sense of Antisense? *Dev. Biol. 243*, 209-214.

(193) Summerton, J., and Weller, D. (1997) Morpholino antisense oligomers: Design, preparation and properties. *Antisense Nucleic Acid Drug Dev. 7*, 187-195.

(194) Stec, W. J., Zon, G., Egan, W., and Stec, B. (1984) Automated solid-phase synthesis, separation, and stereochemistry of phosphorothioate analogs of oligodeoxyribonucleotides. *J. Am. Chem. Soc. 127*, 6077-6079.

(195) Eckstein, F. (1985) Nucleoside phosphorothioates. *Annu. Rev. Biochem. 54*, 367-402.

(196) Damha, M. J., Wilds, C. J., Noronha, A., Brukner, I., Borkow, G., Arion, D., and Parniak, M. A. (1998) Hybrids of RNA and Arabinonucleic Acids (ANA and 2'F-ANA) Are Substrates of Ribonuclease H. *J. Am. Chem. Soc. 120*, 12976-12977.

(197) Jepsen, J. S., and Wengel, J. (2004) Locked Nucleic Acids: a potent nucleic acid analogue in therapeutics and biotechnology. *Curr. Opin. Drug Discovery Dev. 7*, 188-194.

(198) Petersen, M., Bondensgaard, K., Wengel, J., and Jacobsen, J. P. (2002) Locked Nucleic Acid (LNA) Recognition of RNA: NMR Solution Structures of LNA:RNA Hybrids. *J. Am. Chem. Soc. 124*, 5974-5982.

(199) Petersen, M., Håkansson, A. E., Wengel, J., and Jacobsen, J. P. (2001) alpha-L-LNA (alpha-I-ribo configured locked nucleic acid) recognition of RNA. A study by NMR spectroscopy and molecular dynamics simulations. *J. Am. Chem. Soc. 123*, 7431-7432.

(200) Petersen, M., and Wengel, J. (2003) LNA: a versatile tool for therapeutics and genomics. *Trends Biotechnol. 21*, 74-81.

(201) Vester, B., and Wengel, J. (2004) LNA (Locked Nucleic Acid): High-Affinity Targeting of Complementary RNA and DNA. *Biochemistry 43*, 13233-13241.

(202) Amirkanov, N. V., Pradeepkumar, P. I., and Chattopadhyaya, J. (2002) Kinetic analysis of the RNA cleavage of the conformationally-constrained oxetane-modified antisense-RNA hybrid duplex by RNase H. *J. Chem. Soc. Perkin Trans. 2*, 976-984.

(203) Opalinska, J. B., Kalota, A., Gifford, L. K., Lu, P., Jen, K.-Y., Pradeepkumar, P. I., Barman, J., Kim, T. K., Swider, C. R., Chattopadhyaya, J., and Gewirtz, A. M. (2004) Oxetane modified, conformationally constrained, antisense oligodeoxyribonucleotides function efficiently as gene silencing molecules. *Nucl. Acids Res. 32*, 5791-5799.

(204) Pradeepkumar, P. I., Amirkanov, N. V., and Chattopadhyaya, J. (2003) Antisense oligonucleotides with oxetane-constrained cytidine enhance heteroduplex stability, and elicit satisfactory RNase H response as well as

showing improved resistance to both exo and endonucleases. *Org. Biomol. Chem. 1*, 81-92.

(205)   Pradeepkumar, P. I., and Chattopadhyaya, J. (2001) Oxetane modified antisense oligonucleotides promote RNase H cleavage of the complementary RNA strand in the hybrid duplex as efficiently as the native, and offer improved endonuclease resistance. *J. Chem. Soc., Perkin. Trans. 2 11*, 2074-2083.

(206)   Pradeepkumar, P. I., Cheruku, P., Plashkevych, O., Acharya, P., Gohil, S., and Chattopadhyaya, J. (2004) Synthesis, Physicochemical and Biochemical Studies of 1',2'-Oxetane Constrained Adenosine and Guanosine Modified Oligonucleotides, and Their Comparison with Those of the Corresponding Cytidine and Thymidine Analogues. *J. Am. Chem. Soc. 126*, 11484-11499.

(207)   Pradeepkumar, P. I., Zamaratski, E., Foldesi, A., and Chattopadhyaya, J. (2000) Transmission of the conformational information in the antisense/RNA hybrid duplex influences the pattern of the RNase H cleavage reaction. *Tetrahedron Lett. 41*, 8601-8607.

(208)   Pradeepkumar, P. I., Zamaratski, E., Földesi, A., and Chattopadhyaya, J. (2001) Conformation-specific cleavage of antisense oligonucleotide-RNA duplexes by RNase H. *J. Chem. Soc., Perkin. Trans. 2 2*, 402-408.

(209)   Tonkinson, J. L., and Stein, C. A. (1994) Patterns of intracellular compartmentalization, trafficking and acidification of 5'-fluorescein labeled phosphodiester and phosphorothioate oligodeoxynucleotides in HL60 cells. *Nucl. Acids Res. 22*, 4268-4275.

(210)   Marwick, C. (1998) First "antisense" drug will treat CMV retinitis. *J. Am. Med. Assoc. 280*, 867-871.

(211)   Brown, D. A., Kang, S. H., Gryaznov, S. M., DeDionisio, L., Heidenreich, O., Sullivan, S., Xu, X., and Nerenberg, M. I. (1994) Effect of phosphorothioate modification of oligodeoxynucleotides on specific protein binding. *J. Biol. Chem. 269*, 26801-26805.

(212)   Guvakova, M. A., Yakubov, L. A., Vlodavsky, I., Tonkinson, J. L., and Stein, C. A. (1995) Phosphorothioate Oligodeoxynucleotides Bind to Basic Fibroblast Growth Factor, Inhibit Its Binding to Cell Surface Receptors, and Remove It from Low Affinity Binding Sites on Extracellular Matrix. *J. Biol. Chem. 270*, 2620-2627.

(213)   Rockwell, P., O'Connor, W. J., King, K., Goldstein, N. I., Zhang, L. M., and Stein, C. A. (1997) Cell-surface perturbations of the epidermal growth factor and vascular endothelial growth factor receptors by phosphorothioate oligodeoxynucleotides. *Proc. Natl. Acad. Sci. USA 94*, 6523-6528.

(214)   Levin, A. A. (1999) A review of issues in the pharmacokinetics and toxicology of phosphorothioate antisense oligonucleotides. *Biochim. Biophys. Acta 1489*, 69-84.

(215)   Fennewald, S. M., and Rando, R. F. (1995) Inhibition of high affinity basic fibroblast growth factor binding by oligonucleotides. *J. Biol. Chem. 270*, 21718-21721.

(216)   Khaled, Z., Benimetskaya, L., Zeltser, R., Khan, T., Sharma, H. W., Narayanan, R., and Stein, C. A. (1996) Multiple mechanisms may contribute to

the cellular anti-adhesive effects of phosphorothioate oligodeoxynucleotides. *Nucl. Acids Res. 24*, 737-745.

(217)   Benimetskaya, L., Loike, J. D., Khaled, Z., Loike, G., Silverstein, S. C., Cao, L., Khoury, J. E. L., CaI, T.-Q., and Stein, C. A. (1997) Mac-1 (CD11b/CD18) is an oligodeoxynucleotide-binding protein. *Nat. Med. 4*, 414-420.

(218)   Yakubov, L., Khaled, Z., Zhang, L. M., Truneh, A., Vlassov, V., and Stein, C. A. (1993) Oligodeoxynucleotides interact with recombinant CD4 at multiple sites. *J. Biol. Chem. 268*, 18818-18823.

(219)   Majumdar, C., Stein, C. A., Cohen, J. S., Broder, S., and Wilson, S. H. (1989) Stepwise mechanism of HIV reverse transcriptase: primer function of phosphorothioate oligodeoxynucleotide. *Biochemistry 28*, 1340-1346.

(220)   Gao, W. Y., Han, F. S., Storm, C., Egan, W., and Cheng, Y. C. (1992) Phosphorothioate oligonucleotides are inhibitors of human DNA polymerases and RNase H: impications for antisense technology. *Mol. Pharmacol. 41*, 223-229.

(221)   Monia, B. P., Lesnik, E. A., Gonzalez, C., Lima, W. F., McGee, D., Guinosso, C. J., Kawasaki, A. M., Cook, P. D., and Freier, S. M. (1993) Evaluation of 2'-modified oligonucleotides containing 2'-deoxy gaps as antisense inhibitors of gene expression. *J. Biol. Chem. 268*, 14514-14522.

(222)   Giles, R. V., and Tidd, D. M. (1992) Increased specificity for antisense oligodeoxynucleotide targeting of RNA cleavage by RNase H using chimeric methylphosphonodiester/phosphodiester structures. *Nucl. Acids Res. 20*, 763-770.

(223)   Agrawal, S., Jiang, Z., Zhao, Q., Shaw, D., Cai, Q., Roskey, A., Channavajjala, L., Saxinger, C., and Zhang, R. (1997) Mixed-backbone oligonucleotides as second generation antisense oligonucleotides: In vitro and in vivo studies. *Proc. Natl. Acad. Sci. USA 94*, 2620-2625.

(224)   Toulmé, J.-J. (2001) New candidates for true antisense. *Nature Biotech. 19*, 17-18.

(225)   Fahmy, R. G., and Khachigian, L. M. (2004) Locked nucleic acid modified DNA enzymes targeting early growth response-1 inhibit vascular smooth muscle cell growth. *Nucl. Acids Res. 32*, 2281-2285.

(226)   Obika, S., Hari, Y., Sugimoto, T., Sekiguchi, M., and Imanishi, T. (2000) Triplex-forming enhancement with high sequence selectivity by single 2'-O,4'-C-methylene bridged nucleic acid (2',4'-BNA) modification. *Tetrahedron Lett. 41*, 8923-8927.

(227)   Obika, S., Uneda, T., Sugimoto, T., Nanbu, D., Minami, T., Doi, T., and Imanishi, T. (2001) 2'-O,4'-C-Methylene bridged nucleic acid (2',4'-BNA): synthesis and triplex-forming properties. *Bioorg. Med. Chem. 9*, 1001-1011.

(228)   Hannon, G. J. (2002) RNA interference. *Nature 418*, 244-251.

(229)   Carthew, R. W. (2001) Gene silencing by double-stranded RNA. *Curr. Opin. Cell. Biol. 13*, 244-248.

(230)   Sijen, T., and Plasterk, R. H. (2003) Transposon silencing in the *Caenorhabditis elegans* germ line by natural RNAi. *Nature 426*, 310-314.

(231)   Nakahara, K., and Carthew, R. W. (2004) Expanding roles for miRNAs and siRNAs in cell regulation. *Curr. Opin. Cell. Biol. 16*, 127-133.

(232)   Buchini, S., and Leumann, C. J. (2003) Recent improvements in antigene technology. *Curr. Op. Chem. Biol. 7*, 717-726.

(233)   Dominick, P. K., and Jarstfer, M. B. (2004) A Conformationally Constrained Nucleotide Analogue Controls the Folding Topology of a DNA G-Quadruplex. *J. Am. Chem. Soc. 126*, 5050-5051.

(234)   Mouritzen, P., Nielsen, A. T., Pfundheller, H. M., Choleva, Y., Kongsbak, L., and Moller, S. (2003) Single nucleotide polymorphism genotyping using locked nucleic acid (LNA). *Expert Rev. Mol. Diagn. 3*, 27-38.

(235)   Letertre, C., Perelle, S., Dilasser, F., Arar, K., and Fach, P. (2003) Evaluation of the performance of LNA and MGB probes in 5'-nuclease PCR assays. *Mol. Cell Probes 17*, 307-311.

(236)   Ugozzoli, L. A., Latorra, D., Pucket, R., Arar, K., and Hamby, K. (2004) Real-time genotyping with oligonucleotide probes containing locked nucleic acids. *Anal. Biochem. 324*, 143-152.

(237)   Jacobsen, N., Nielsen, P. S., Jeffares, D. C., Eriksen, J., Ohlsson, H., Arctander, P., and Kauppinen, S. (2004) Direct isolation of poly(A)+ RNA from 4 M guanidine thiocyanate-lysed cell extracts using locked nucleic acid-oligo(T) capture. *Nucl. Acids Res. 32*, e64.

(238)   Tolstrup, N., Nielsen, P. S., Kolberg, J. G., Frankel, A. M., Vissing, H., and Kauppinen, S. (2003) OligoDesign: Optimal design of LNA (locked nucleic acid) oligonucleotide capture probes for gene expression profiling. *Nucl. Acids Res. 31*, 3758-3762.

(239)   Silahtaroglu, A. N., Tommerup, N., and Vissing, H. (2003) FISHing with locked nucleic acids (LNA): evaluation of different LNA/DNA mixmers. *Mol. Cell Probes 17*, 165-169.

(240)   Denisov, A. Y., Zamaratski, E. V., Maltseva, T. V., Sandström, A., Bekiroglu, S., Altmann, K.-H., Egli, M., and Chattopadhyaya, J. (1998) The Solution Conformation of a Carbocyclic Analog of the Dickerson-Drew Dodecamer: Comparison with its own X-ray Structure and that of the NMR Structure of the Native Counterpart. *J. Biomol. Struct. Dyn. 16*, 547-568.

(241)   Smirnov, S., Johnson, F., Marumoto, R., and de los Santos, C. (2000) Structure of an 11-mer DNA duplex containing the carbocyclic nucleotide analog: 2'-deoxyaristeromycin. *J. Biomol. Struct. Dyn. 17*, 981-991.

(242)   Portmann, S., Altmann, K.-H., Reynes, N., and Egli, M. (1997) Crystal Structures of Oligodeoxyribonucleotides Containing 6'-a-Methyl and 6'-a-Hydroxy Carbocyclic Thymidines. *J. Am. Chem. Soc. 119*, 2396-2403.

(243)   Kalman, A., Koritsanszky, T., Beres, J., and Sagi, G. Crystal and molecular structure of (+)-carba-thymidine, $C_{11}H_{16}N_2O_4$. *Nucleosides & Nucleotides 9*, 235-243.

(244)   Kusaka, T., Yamamoto, H., Shibata, M., Muroi, M., Kishi, T., and Mizuno, K. (1968) Streptomyces citricolor and a new antibiotic, aristeromycin. *J. Antibiot. 21*, 255-263.

(245)   Thibaudeau, C., Kumar, A., Bekiroglu, S., Matsuda, A., Marquez, V. E., and Chattopadhyaya, J. (1998) NMR Conformation of (-)-β-D-

Aristeromycin and Its 2'-Deoxy and 3'-Deoxy Counterparts in Aqueous Solution. *J. Org. Chem. 63*, 5447-5462.

(246)   Dickerson, R. E., and Drew, H. R. (1981) Structure of a B-DNA dodecamer: II. Influence of base sequence on helix structure. *J. Mol. Biol. 149*, 761-786.

(247)   Drew, H. R., Wing, R. M., Takano, T., Broka, C., Tanaka, S., Itakura, K., and Dickerson, R. E. (1981) Structure of a B-DNA Dodecamer: Conformation and Dynamics. *Proc. Natl. Acad. Sci. USA 78*, 2179-2183.

(248)   Hakoshima, T., Fukui, T., Ikehara, M., and Tomita, K.-I. (1981) Molecular structure of a double helix that has non-Watson-Crick type base pairing formed by 2-substituted poly(A) and poly(U). *Proc. Natl. Acad. Sci. USA 78*, 7309-7313.

(249)   Abrescia, N. G. A., Thompson, A., Huynh-Dinh, T., and Subirana, J. A. (2002) Crystal structure of an antiparallel DNA fragment with Hoogsteen base pairing. *Proc. Natl. Acad. Sci. USA 99*, 2806-2811.

(250)   Nair, D. T., Johnson, R. E., Prakash, S., Prakash, L., and Aggarwal, A. K. (2004) Replication by human DNA polymerase-ι occurs by Hoogsteen base-pairing. *Nature 430*, 377-380.

(251)   Hrebabecky, H., and Farkas, J. (1974) Nucleic acid components and their analogs. CLXVI. Synthesis of 7- and 9β-D-psicofuranosylguanine and their 1'-deoxy derivatives. *Collect. Czech. Chem. Commun. 39*, 2115-2123.

(252)   Dobson, C. M., Lian, L.-Y., Redfield, C., and Topping, K. D. (1986) Measurement of Hydrogen Exchange Rates Using 2D NMR Spectroscopy. *J. Magn. Reson. 69*, 201-209.

(253)   Wärmländer, S., Sponer, J. E., Sponer, J., and Leijon, M. (2002) The Influence of the Thymine C5 Methyl Group on Spontaneous Base Pair Breathing in DNA. *J. Biol. Chem. 277*, 28491-28497.

(254)   Núñez, M. E., and Barton, J. K. (2000) Probing DNA charge transport with metallointercalators. *Curr. Op. Chem. Biol. 4*, 199-206.

(255)   Boon, E. M., Ceres, D. M., Drummond, T. G., Hill, M. G., and Barton, J. K. (2000) Mutation detection by electrocatalysis at DNA-modified electrodes. *Nature Biotechnol. 18*, 1096-1100.

(256)   Boon, E. M., Salas, J. E., and Barton, J. K. (2002) An electrical probe of protein–DNA interactions on DNA-modified surfaces. *Nature Biotechnol. 20*, 282-286.

(257)   Simpkins, H., and Richards, E. G. (1967) Titration Properties of Some Dinucleotides. *Biochemistry 6*, 2513-2520.

(258)   Vesnaver, G., and Breslauer, K. J. (1991) The contribution of DNA single-stranded order to the thermodynamics of duplex formation. *Proc. Natl. Acad. Sci. USA 88*, 3569-3573.

(259)   Filimonov, V. V., and Privalov, P. L. (1977) Thermodynamics of base interaction in (A)$_n$ and (A·U)$_n$. *J. Mol. Biol. 122*, 465-470.

(260)   Suurkuusk, J., Alvarez, J., Freire, E., and Biltonen, R. (1977) Calorimetric determination of the heat capacity changes associated with the conformational transitions of polyriboadenylic acid and polyribouridylic acid. *Biopolymers 16*, 2641-2652.

(261) Olsthoorn, S. M., Bostelaar, L. J., DeRooij, J. F. M., Van Boom, J. H., and Altona, C. (1981) Circular Dichroism Study of Stacking Properties of Oligodeoxyadenylates and Polydeoxyadenylate. *Eur. J. Biochem. 115*, 309-321.

(262) Powell, J. T., Richards, E. G., and Gratzer, W. B. (1972) The Nature of Stacking Equilibria in Polynucleotides. *Biopolymers 11*, 235-250.

(263) Warshaw, M. M., and Tinoco, I. J. (1965) Absorption and optical rotatory dispersion of six dinucleoside phosphates. *J. Mol. Biol. 13*, 54-64.

(264) Simkins, H., and Richards, E. G. (1967) Preparation and properties of oligouridylic acids. *J. Mol. Biol. 29*, 349-356.

(265) Richards, E. G., Flessel, P., and Fresco, J. R. (1963) Polynucleotides. VI. Molecular properties and conformation of polyribouridylic acid. *Biopolymers 1*, 431-446.

(266) Inners, L. D., and Felsenfeld, G. (1970) Conformation of polyribouridylic acid in solution. *J. Mol. Biol. 50*, 373-389.

(267) Broom, A. D., Schweizer, M. P., and Ts'o, P. O. P. (1967) Interaction and association of bases and nucleosides in aqueous solutions. V. Studies of the association of purine nucleosides by vapor pressure osmometry and by proton magnetic resonance. *J. Am. Chem. Soc. 89*, 3612-3622.

(268) Chan, S. I., and Nelson, J. H. (1969) Proton magnetic resonance studies of ribose dinucleoside monophosphates in aqueous solution. I. Nature of the base-stacking interaction in adenylyl(3'->5')adenosine. *J. Am. Chem. Soc. 91*, 168-183.

(269) Lee, C.-H., Ezra, F. S., Kondo, N. S., Sarma, R. H., and Danyluk, S. S. (1976) Conformational properties of dinucleoside monophosphates in solution: dipurines and dipyrimidines. *15*, 3627-3639.

(270) Kolodny, N. H., and Neville, A. C. (1980) Effects of pD on ring-stacking interactions between dinucleoside phosphates and tryptamine. *Biopolymers 19*, 2223-2245.

(271) Lee, C.-H., and Tinoco, I. J. (1980) Conformation studies of 13 trinucleoside diphosphates by 360 MHz PMR spectroscopy. a bulged base conformation: I. base protons and H1' protons. *Biophys. Chem. 11*, 283-294.

(272) van den Hoogen, Y. T., Erkelens, C., de Vroom, E., van der Marel, G. A., van Boom, J. H., and Altona, C. (1988) Influence of uracil on the conformational behaviour of RNA oligonucleotides in solution. *Eur. J. Biochem. 173*, 295-303.

(273) Freier, S. M., Burger, B. J., Alkema, D., Neilson, T., and Turner, D. H. (1983) Effects of 3' Dangling End Stacking on the Stability of GGCC and CCGG Double Helices. *Biochemistry 22*, 6198-6206.

(274) Freier, S. M., Alkema, D., Sinclair, A., Neilson, T., and Turner, D. H. (1985) Contributions of Dangling End Stacking and Terminal Base-Pair Formation to the Stabilities of XGGCCp, XCCGGp, XGGCCY, and XCCGGYp Helixes. *Biochemistry 24*, 4533-4539.

(275) Freier, S. M., Sugimoto, N., Sinclair, A., Alkema, D., Neilson, T., Kierzek, R., Caruthers, M. H., and Turner, D. H. (1986) Stability of XGCGCp, GCGCYp and XGCGCYp Helixes: An Emperical Estimate of the Energetics of Hydrogen Bonds in Nucleic Acids. *Biochemistry 25*, 3214-3219.

72

(276) Turner, D. H., Sugimoto, N., and Freier, S. M. (1988) RNA Structure Prediction. *Ann. Rev. Biophys. Biophys. Chem. 17*, 167-192.

(277) Sugimoto, N., Kierzek, R., and Turner, D. H. (1987) Sequence Dependence for the Energetics of Dangling Ends and Terminal Base Pairs in Ribonucleic Acid. *Biochemistry 26*, 4554-4558.

(278) Turner, D. H., Sugimoto, N., Kierzek, R., and Dreiker, S. D. (1987) Free Energy Increments for Hydrogen Bonds in Nucleic Acid Base Pairs. *J. Am. Chem. Soc. 109*, 3783-3785.

(279) Luo, R., Gilson, H. S. R., Potter, M. J., and Gilson, M. K. (2001) The Physical Basis of Nucleic Acid Base Stacking in Water. *Biophys. J. 80*, 140-148.

(280) Friedman, R. A., and Honig, B. (1995) A free energy analysis of nucleic acid base stacking in aqueous solution. *Biophys. J. 69*, 1528-1535.

(281) Jencks, W. P. (1975) Binding energy, specificity, and enzymic catalysis: the Circe effect. *Adv. Enzymol. 43*, 219-410.

(282) Narlikar, G. J., and Herschlag, D. (1997) MECHANISTIC ASPECTS OF ENZYMATIC CATALYSIS: Lessons from Comparison of RNA and Protein Enzymes. *Ann. Rev. Biochem. 66*, 19-59.

(283) Legault, P., and Pardi, A. (1994) In Situ Probing of Adenine Protonation in RNA by [13]C. *J. Am. Chem. Soc. 116*, 8390-8391.

(284) Legault, P., and Pardi, A. (1997) Unusual Dynamics and pK_a Shift at the Active Site of a Lead-Dependent Ribozyme. *J. Am. Chem. Soc. 119*, 6621-6628.

(285) Ravindranathan, S., Butcher, S. E., and Feigon, J. (2000) Adenine Protonation in Domain B of the Hairpin Ribozyme. *Biochemistry 39*, 16026-16032.

(286) Muth, G. W., Ortoleva-Donnelly, L., and Strobel, S. A. (2000) A Single Adenosine with a Neutral pKa in the Ribosomal Peptidyl Transferase Center. *Science 289*, 949-950.

(287) Xiong, L., Polacek, N., Sander, P., Böttger, E. C., and Mankin, A. (2001) pK_a of adenine 2451 in the ribosomal peptidyl transferase center remains elusive. *RNA 7*, 1365-1369.

(288) Drohat, A. C., and Stivers, J. T. (2000) NMR Evidence for an Unusually Low N1 pK_a for Uracil Bound to Uracil DNA Glycosylase: Implications for Catalysis. *J. Am. Chem. Soc. 122*, 1840-1841.

(289) Drohat, A. C., and Stivers, J. T. (2000) *Escherichia coli* Uracil DNA Glycosylase: NMR Characterization of the Short Hydrogen Bond from His187 to Uracil O2. *Biochemistry 39*, 11865-11875.

(290) Nakano, S.-i., Chadalavada, D. M., and Bevilacqua, P. C. (2000) General Acid-Base Catalysis in the Mechanism of a Hepatitis Delta Virus Ribozyme. *Science 287*, 1493-1497.

(291) Lupták, A., Ferré-D´Amaré, A. R., Zhou, K., Zilm, K. W., and Doudna, J. A. (2001) Direct pK_a Measurement of the Active-Site Cytosine in a Genomic Hepatitis Delta Virus Ribozyme. *J. Am. Chem. Soc. 123*, 8447-8452.

(292) Perrotta, A. T., Shih, I.-h., and Been, M. D. (1999) Imidazole Rescue of a Cytosine Mutation in a Self-Cleaving Ribozyme. *Science 286*, 123-126.

(293) Wang, C., Gao, H., Gaffney, B. L., and Jones, R. A. (1991) Nitrogen-15-Labeled Oligodeoxynucleotides. 3. Protonation of the Adenine N1 in the

A•C and A•G Mispairs of the Duplexes {d[CG($^{15}N^1$)AGAATTCCCG]}$_2$ and {d[CGGGAATTC($^{15}N^1$)ACG]}$_2$. *J. Am. Chem. Soc. 113*, 5486-5488.

(294) Boulard, Y., Cognet, J. A., Gabarro-Arpa, J., Le Bret, M., Sowers, L. C., and Fazakerley, G. V. (1992) The pH dependent configurations of the C.A mispair in DNA. *Nucl. Acids Res. 20*, 1933-1941.

(295) Cai, Z., and Tinoco, I. J. (1996) Solution Structure of Loop A from the Hairpin Ribozyme from Tobacco Ringspot Virus Satellite. *Biochemistry 35*, 6026-6036.

(296) Doherty, E., and Doudna, J. A. (2000) Ribozyme Structures and Mechanisms. *Annu. Rev. Biochem. 69*, 597-615.

(297) Acharya, P., Acharya, S., Cheruku, P., Amirkhanov, N. V., Földesi, A., and Chattopadhyaya, J. (2003) Cross-Modulation of the pKa of Nucleobases in a Single-Stranded Hexameric-RNA Due to Tandem Electrostatic Nearest-Neighbor Interactions. *J. Am. Chem. Soc. 125*, 9948-9961.

(298) Acharya, P., Acharya, S., Földesi, A., and Chattopadhyaya, J. (2003) Tandem Electrostatic Effect from the First to the Third Aglycon in the Trimeric RNA Owing to the Nearest-Neighbor Interaction. *J. Am. Chem. Soc. 125*, 2094-2100.

(299) Acharya, P., Cheruku, P., Chatterjee, S., Babu Karthick, S., Acharya, S., and Chattopadhyaya, J. (2004) The Measurement of Nucleobase pKa of the Model Mononucleotides shows why RNA-RNA duplex is more stable than DNA-DNA duplex. *J. Am. Chem. Soc. 126*, 2862-2869.

(300) Acharya, P., Trifonova, A., Thibaudeau, C., Földesi, A., and Chattopadhyaya, J. (1999) The transmission of the electronic character of guanine-9-yl the sugar-phosphate backbone torsions in guanosine 3',5'-bisphosphate. *Angew. Chem. Int. Ed. 38*, 3645-3650.

(301) Acharya, S., Acharya, P., Földesi, A., and Chattopadhyaya, J. (2003) Cross-Modulation of Physicochemical Character of Aglycones in Dinucleoside (3'->5') Monophosphates by the Nearest Neighbor Interaction in the Stacked State. *J. Am. Chem. Soc. 124*, 13722-13730.

(302) Rooman, M., Liévin, J., Buisine, E., and Wintjens, R. (2002) Cation-π/H-bond Stair Motifs at Protein–DNA Interfaces. *J. Mol. Biol. 319*, 67-76.

(303) Jones, G. B. (2001) π Shielding in organic synthesis. *Tetrahedron 57*, 7999-8016.

(304) Jones, G. B., and Chapman, B. J. (1995) π Stacking Effects in Asymmetric Synthesis. *Synthesis*, 475-497.

(305) Yamada, S., and Morita, C. (2002) Face-Selective Addition to a Cation-Complex of a Pyridinium Salt: Synthesis of Chiral 1,4-Dihydropyridines. *J. Am. Chem. Soc. 124*, 8184-8185.

(306) Limmer, S., Hofmann, H.-P., Ott, G., and Sprinzl, M. (1993) The 3'-terminal end (NCCA) of the tRNA determines the structure and stability of the aminoacul acceptor stem. *Proc. Natl. Acad. Sci. 90*, 6199-6202.

(307) Nagan, M. C., Beuning, P., Musier-Forsyth, K., and Cramer, C. J. (2000) Importance of discriminator base stacking interactions: molecular dynamics analysis of A73 microhelix[Ala] variants. *Nucl. Acids Res. 28*, 2527-2534.

(308) Alkema, D., Bell, R. A., Hader, P. A., and Neilson, T. (1981) Invariant Adenosine Residues Stabilize tRNA D Stems. *Fed. Euro. Biochem. Soc. Letters 136*, 70-71.

(309) Yoon, K., Turner, D. H., Tinoco, I. J., Haar, F., and Cramer, F. (1976) The kinetics of binding of U-U-C-A to a dodecanucleotide anticodon fragment from yeast tRNA-Phe. *Nucl. Acids Res. 3*, 2233-2241.

(310) Ayer, D., and Yarus, M. (1986) The context effect does not require a fourth base pair location. *Science 231*, 393-395.

(311) Elbashir, S. M., Harborth, J., Lendeckel, W., Yalcin, A., Weber, K., and Tuschl, T. (2001) Duplexes of 21-nucleotide RNAs mediate RNA interference in cultured mammalian cells. *Nature 411*, 494-498.

(312) Elbashir, S. M., Lendeckel, W., and Tuschl, T. (2001) RNA interference is mediated by 21- and 22-nucleotide RNAs. *Genes. dev 15*, 188-200.

(313) Amarzguioui, M., and Prydz, H. (2004) An algorithm for selection of functional siRNA sequences. *Biochem. biophys. res. comm. 316*, 1050-1058.

(314) Ma, J.-B., Ye, K., and Patel, D. J. (2004) Structural basis for overhang-specific small interfering RNA recognition by the PAZ domain. *Nature 429*, 318-322.

(315) Martin, F. H., Uhlenbeck, O. C., and Doty, P. (1971) Self-complementary oligoribonucleotides: Adenylic acid-uridylic acid block copolymers. *J. Mol. Biol. 57*, 201-215.

(316) Uhlenbeck, O. C., Martin, F. H., and Doty, P. (1971) Self-complementary oligoribonucleotides: Effects of helix defects and guanylic acid-cytidylic acid base pairs. *J. Mol. Biol. 57*, 217-229.

(317) Romaniuk, P. J., Hughes, D. W., Gregoire, R. J., Neilson, T., and Bell, R. A. (1978) Stabilizing Effect of Dangling Bases on a Short RNA Double Helix as Determined by Proton Nuclear Magnetic Resonance Spectroscopy. *J. Am. Chem. Soc. 100*, 3971-3972.

(318) Neilson, T., Romaniuk, P. J., Alkema, D., Hughes, D. W., Evertt, J. R., and Bell, R. A. (1980) The effects of base sequence and dangling bases on the stability of short ribonucleic acid duplexes. *Nucl. Acids Symp. Ser. 7*, 293-311.

(319) Bommarito, S., Peyret, N., and SantaLucia Jr, J. (2000) Thermodynamic parameters of DNA sequences with dangling ends. *Nucl. Acids Res. 28*, 1929-1934.

(320) Ohmichi, T., Nakano, S.-i., Miyoshi, D., and Sugimoto, N. (2002) Long RNA Dangling End Has Large Energetic Contribution to Duplex Stability. *J. Am. Chem. Soc. 124*, 10367-10372.

(321) Burkard, M. E., Kierzek, R., and Turner, D. H. (1999) Thermodynamics of Unpaired Terminal Nucleotides on Short RNA Helixes Correlates with Stacking at Helix Termini in Larger RNAs. *J. Mol. Biol. 290*, 967-982.

(322) Rosemeyer, H., and Seela, F. (2002) Modified purine nucleosides as dangling ends of DNA duplexes: the effect of the nucleobase polarizability on stacking interactions. *J. Chem. Soc. Perklin Trans. 2*, 746-750.

(323) Tuma, J., Connors, W. H., Stitelman, D. H., and Richert, C. (2002) On the Effect of Covalently Appended Quinolones on Termini of DNA duplexes. *J. Am. Chem. Soc. 124*, 4236-4246.

(324)   Ziomek, K., Kierzek, E., Biala, E., and Kierzek, R. (2002) The influence of various modified nucleotides placed as 3'-dangling end on thermal stability of RNA duplexes. *Biophys. Chem. 97*, 243-249.

(325)   Ziomek, K., Kierzek, E., Biala, E., and Kierzek, R. (2002) The termal stability of RNA duplexes containing modified base pairs placed at internal and terminal positions of the oligoribonucleotides. *Biophys. Chem. 97*, 233-241.

(326)   Nakano, S.-i., Uotani, Y., Nakashima, S., Anno, Y., Fujii, M., and Sugimoto, N. (2003) Large Stabilization of a DNA duplex by the Deoxyadenosine Derivatives Tethering an Aromatic Hydrocarbon Group. *J. Am. Chem. Soc. 125*, 8086-8087.

(327)   Guckian, K. M., Schweizer, B. A., Ren, R. X.-F., Sheils, C. J., Paris, P. L., Tahmassebi, D. C., and Kool, E. T. (1996) Experimental Measurement of Aromatic Stacking Affinities in the Context of Duplex DNA. *J. Am. Chem. Soc. 118*, 8182-8183.

(328)   Maltseva, T., Agback, P., Repkova, M. N., Venyaminova, A. G., Ivanova, I. M., Sandström, A., Zarytova, V. F., and Chattopadhyaya, J. (1994) The solution structure of a 3'-phenazinium (Pzn) tethered DNA-RNA duplex with a dangling adenosine: r(5'G-AUUGAA3'):d(5'TCAATC3'-Pzn). *Nucl. Acids Res. 22*, 5590-5599.

(329)   Bleczinski, C. F., and Richert, C. (1999) Steroid-DNA Interactions Increasing Stability, Sequence-Selectivity, DNA/RNA Discrimination and Hypochromicity of Oligonucleotide Duplexes. *J. Am. Chem. Soc. 121*, 10889-10894.

(330)   Tuma, J., and Richert, C. (2003) Solution Structure of a Steroid-DNA Complex with Cholic Acid Residues Sealing the Termini of a Watson-Crick Duplex. *Biochemistry 42*, 8957-8965.

(331)   Mokhir, A. A., Tetzlaff, C. N., Herzberger, S., Mosbacher, A., and Richert, C. (2001) Monitored Selection of DNA-hybrids Forming Duplexes with Capped Terminal C:G Pairs. *J. Comb. Chem. 3*, 374-386.

(332)   Znosko, B. M., Burkard, M. E., Krugh, T. R., and Turner, D. H. (2002) Molecular Recognition in Purine-Rich Internal Loops: Thermodynamic, Structural and Dynamic Consequences of Purine for Adenine Substitutions in 5'(rGGCAAGCCU)$_2$. *Biochemistry 41*, 14978.

(333)   Lane, A., Martin, S. R., Ebel, S., and Brown, T. (1992) Solution Conformation of a Deoxynucleotide Containing Tandem G-A Mismatched Base Pairs and 3'-Overhanding Ends in d(GTGAACTT)$_2$. *Biochemistry 31*, 12087-12095.

(334)   Breslauer, K. J., Frank, R., Heikens, W., Blöcker, H., and Marky, L. A. (1986) Predicting DNA duplex stability from the base sequence. *Proc. Natl. Acad. Sci. 83*, 3746-3750.

(335)   SantaLucia Jr, J., Allawi, H. T., and Seneviratne, P. A. (1996) Improved Nearest-Neighbor Parameters for Predicting DNA Duplex Stability. *Biochemistry 35*, 3555-3562.

(336)   Gray, D. M. (1997) Derivation of Nearest-Neighbor Properties from Data on Nucleic Acid Oligomers. I. Simple Sets of Independent Sequences and the Influence of Absent Nearest Neighbors. *Biopolymers 42*, 783-793.

(337)   Xia, T., SantaLucia Jr, J., Burkard, M. E., Kierzek, R., Schroeder, S. J., Jiao, X., Cox, C., and Turner, D. H. (1998) Thermodynamic Parameters for an Expanded Nearest-Neighbor Model for Formation of RNA Duplex with Watson-Crick Base Pairs. *Biochemistry 37*, 14719-14735.

(338)   Mathews, D. H., Sabina, J., Zuker, M., and Turner, D. H. (1999) Expanded Sequence Dependence of Thermodynamic Parameters Improves Prediction of RNA Secondary Structure. *J. Mol. Biol. 288*, 911-940.

(339)   Ma, L., Cheng, C., Miyajima, H., Zhao, Y., and Herdewijn, P. (2002) Predicting melting temperature (Tm) of oligoribonucleotide duplex by neural network. *J. Chemometrics 16*, 75-80.

(340)   SantaLucia Jr, J., and Hicks, D. (2004) The Thermodynamics of DNA Structural Motifs. *Annu. Rev. Biophys. Biomol. Struct. 33*, 415-440.

(341)   Zuker, M. (2003) Mfold web server for nucleic acid folding and hybridization prediction. *Nucl. Acids Res. 31*, 3406-3415.

(342)   SantaLucia Jr, J. (1998) A unified view of polymer, dumbbell, and oligonucleotide DNA nearest-neighbor thermodynamics. *Proc. Natl. Acad. Sci. 95*, 1460-1465.

(343)   Bhattacharya, P. K., Cha, J., and Barton, J. K. (2002) 1H NMR determination of base-pair lifetimes in oligonucleotides containing single base mismatches. *Nucl. Acids Res. 30*, 4740-4750.

(344)   Kim, J., Walter, A. E., and Turner, D. H. (1996) Thermodynamics of Coaxially Stacked Helixes with GA and CC Mismatches. *Biochemistry 35*, 13753-13761.

(345)   Peyret, N., Seneviratne, P. A., Allawi, H. T., and SantaLucia, J., Jr. (1999) Nearest-Neighbor Thermodynamics and NMR of DNA Sequences with Internal A×A, C×C, G×G, and T×T Mismatches. *Biochemistry 38*, 3468-3477.

(346)   Kool, E. T. (2000) Synthetically modified DNAs as substrates for polymerases. *Curr. Opin. Chem. Biol. 4*, 602-608.

Acta Universitatis Upsaliensis

*Digital Comprehensive Summaries of Uppsala Dissertations
from the Faculty of Science and Technology* 71

Editor: The Dean of the Faculty of Science and Technology

A doctoral dissertation from the Faculty of Science and
Technology, Uppsala University, is usually a summary of a
number of papers. A few copies of the complete dissertation
are kept at major Swedish research libraries, while the
summary alone is distributed internationally through the
series Digital Comprehensive Summaries of Uppsala
Dissertations from the Faculty of Science and Technology.
(Prior to January, 2005, the series was published under the
title "Comprehensive Summaries of Uppsala Dissertations
from the Faculty of Science and Technology".)